Research Paper

GEOSPHERE

GEOSPHERE, v. 19, no. 2

https://doi.org/10.1130/GES02541.1

10 figures; 2 tables; 1 set of supplemental files

CORRESPONDENCE: tysn.smth@gmail.com

CITATION: Smith, T.M., Saylor, J.E., Lapen, T.J., Hatfield, K., and Sundell, K.E., 2023, Identifying sources of non-unique detrital age distributions through integrated provenance analysis: An example from the Paleozoic Central Colorado Trough: Geosphere, v. 19, no. 2, p. 471–492, https://doi.org/10.1130/GES02541.1.

Science Editor: Andrea Hampel
Associate Editor: Cathy Busby

Received 21 April 2022
Revision received 13 September 2022
Accepted 7 October 2022

Published online 18 January 2023

Identifying sources of non-unique detrital age distributions through integrated provenance analysis: An example from the Paleozoic Central Colorado Trough

Tyson M. Smith[1,*], Joel E. Saylor[2], Tom J. Lapen[1], Kendall Hatfield[1], and Kurt E. Sundell[3,†]

[1]Department of Earth and Atmospheric Sciences, University of Houston, Houston, Texas 77204, USA
[2]Department of Earth, Ocean, and Atmospheric Sciences, University of British Columbia, Vancouver, British Columbia V6T1Z4, Canada
[3]Department of Geosciences, University of Arizona, Tucson, Arizona 85721, USA

ABSTRACT

To address the longstanding issue of provenance interpretation of non-unique detrital zircon age populations, we integrated zircon U-Pb, rare earth element (REE), and εHf(t) data from upper Paleozoic strata in the northern Central Colorado Trough and Cambrian intrusions with petrography, paleocurrent data, and structural and stratigraphic observations. This data set indicates that Cambrian sediment was shed by multiple local sources instead of distant sources hundreds of kilometers away, and it reveals a detailed history of tectonic drainage reorganization in the northern Central Colorado Trough during Ancestral Rocky Mountain deformation. During the Early–Middle Pennsylvanian, Cambrian detrital zircons were a minor constituent of northern Central Colorado Trough sediment. However, during the Late Pennsylvanian–early Permian, westward advancement of the adjacent Apishapa Uplift deformation front precipitated drainage reorganization, which resulted in an episode of dominant Cambrian detrital zircon sourcing. Paleocurrent and petrographic data indicate that the source of Cambrian detritus was shed by an igneous rock body that was ≤15 km northeast of the depocenter, which has since been eroded away or mantled by Tertiary volcanic rocks. The addition of zircon petrochronology to the data set applied here was critical in confirming this hidden source of detritus and elucidating the compositional characteristics of that igneous rock. Zircon εHf(t) provided a regional provenance indicator of a western Laurentian affinity, and REE composition aided in discriminating possible local sources of Cambrian zircon. Furthermore, this work serves as a case study of a dominant Cambrian detrital zircon signature sourced from outside of the well-known Amarillo-Wichita Uplift, and it has implications for the interpretation of such detrital spectra in the context of a direct-from-basement source or the recycling of Cambrian zircon-dominated rocks. In summary, we demonstrate the utility of this multi-provenance proxy approach in interpreting a complex structural history of a dynamic hinterland and concomitant drainage reorganization through an in-depth investigation into the basin record.

Tyson Smith https://orcid.org/0000-0003-2834-3526
*Now at Geosciences and Environmental Change Science Center, U.S. Geologic Survey, Denver Federal Center, Denver, Colorado 80225, USA
†Now at Department of Geosciences, Idaho State University, Pocatello, Idaho 83209, USA

INTRODUCTION

Similar ages in disparate sediment sources complicate analyses of detrital zircon age spectra and can make provenance interpretation equivocal. One example of this dilemma comes from upper Paleozoic strata associated with the Ancestral Rocky Mountains, which contain, and at times are dominated by, Cambrian zircons (Leary et al., 2020). When found in strata in the midcontinent and western North America, these ages are commonly attributed to sources in the Amarillo-Wichita Uplift of southern Oklahoma and northern Texas, which was exhumed during Ancestral Rocky Mountain deformation (e.g., Dickinson et al., 2010). However, other possible sources include smaller outcrops of Cambrian igneous rocks that are exposed throughout Colorado and New Mexico (Larson et al., 1985; McMillan and McLemore, 2004), which have been considered to be possible sediment sources by other authors (e.g., Rasmussen and Foreman, 2017; Ejembi et al., 2021). Recycling of Paleozoic strata is yet another possible source, as some of these sedimentary rocks contain abundant Cambrian zircons (e.g., Amato and Mack, 2012).

Detrital zircon trace-element and isotopic compositions are increasingly being used in provenance analysis to augment U-Pb ages and mitigate the uncertainty of nonunique age distributions (e.g., strata in the Cenozoic Altiplano; Sundell et al., 2019). Variations in zircon Hf isotopes and rare-earth elements (REE) are related to the evolution of magmatic sources (e.g., Belousova et al., 2010) and parent rock-type (Belousova et al., 2002), respectively, and can therefore be used as additional fingerprints of provenance. We endeavor to characterize this behavior in zircons from North American Cambrian igneous rocks as they indeed vary in associated rock type, and magmatic history, including the age of crust into which they were emplaced. Further, we compare zircon REE and Hf-isotopic records from Cambrian-aged detrital and igneous zircon samples to aid in provenance discrimination between potential sources. In applying these techniques to Cambrian detrital zircons in Central Colorado Trough strata, we find that zircon petrochronology yields critical insights into the nature and evolution of the sediment source area. However, we also find the integration of multiple provenance proxies, along with these zircon data, to be critical as well. There is no silver bullet in provenance discrimination.

We present new detrital zircon U-Pb data from the Central Colorado Trough that are dominated by Cambrian ages, the source of which are unknown. To discriminate between potential sources of Cambrian detrital zircon in Central Colorado Trough strata, our provenance analysis approach includes zircon U-Pb, εHf(t), and REE composition, as well as paleocurrent measurements, sandstone petrography, and the incorporation of structural and stratigraphic data. Evaluation of all of these data in concert was critical in developing and testing hypotheses of source area evolution, and in reconstructing episodes of drainage reorganization in this Ancestral Rocky Mountain basin.

GEOLOGIC SETTING

Upper Paleozoic–lower Mesozoic strata in the Central Colorado Trough and Eagle Basin contain Cambrian detrital zircons, which have multiple potential igneous and sedimentary sources across North America (e.g., Dickinson et al., 2010; Amato and Mack, 2012; Link et al., 2017; Ejembi et al., 2021). However, igneous sources are of particular interest for several reasons. (1) Cambrian igneous rocks are widely distributed across middle and western North America but are volumetrically limited in comparison to other Laurentia crustal ages (Whitmeyer and Karlstrom, 2007); (2) the initial igneous source of earlier Paleozoic rocks that could have been recycled into Central Colorado Trough strata yields sedimentary source information, albeit indirectly; and (3) Ancestral Rocky Mountain basin strata are commonly arkosic, particularly grading upsection (e.g., Kottlowski, 1961; Kluth and Coney, 1981; Suttner and Dutta, 1986; Johnson et al., 1992; Musgrave, 2003), which indicates a strong basement component of sediment source. Furthermore, the colocation of Cambrian igneous rocks and late Paleozoic intraplate exhumation is not purely coincidental. These Cambrian igneous rocks were emplaced during the rifting of Rodinia (McMillan and McLemore, 2004; Keller and Stephenson, 2007; Hanson et al., 2013), and subsequent Ancestral Rocky Mountain deformation was strongly influenced by many of these pre-existing faults and zones of weakness (Marshak et al., 2000; Soreghan et al., 2012; Leary et al., 2017).

Ancestral Rocky Mountains and the Central Colorado Trough

The Ancestral Rocky Mountains are the result of late Paleozoic basement-involved intraplate deformation (Kluth and Coney, 1981). They exhibit predominantly northwest-trending structures (modern reference frame), span from the midcontinent to western Laurentia, and developed during the most recent episode of supercontinent accretion, when the eastern, western, and southern Laurentian margins were tectonically active (Kluth and Coney, 1981; Kluth, 1986; Ye et al., 1996; Leary et al., 2017). The core of Ancestral Rocky Mountain deformation occurred along the pre-existing transcontinental arch (Fig. 1; Leary et al., 2017), which itself was a long-lived, northeast–southwest-trending lithospheric structure that affected sedimentation throughout most of the Paleozoic (e.g., Carlson, 1999; Linde et al., 2014). The precise outlines of Ancestral Rocky Mountain uplifts are uncertain in many locations due to subsequent episodes of magmatism and deformation that overprinted many Ancestral Rocky Mountain features (Kluth, 1997). However, syndepositional strata and Ancestral Rocky Mountain structures that are preserved present a preliminary template from which to interpret the shape of these uplifts (Fig. 2) and the nature of deformation, which was dominated by basement-seated reverse and thrust faulting (e.g., Frahme and Vaughn, 1983; Baltz and Meyers, 1999; Hoy and Ridgeway, 2002; Thomas, 2007; Timbel, 2015). This shortening and consequent lithospheric flexure drove accommodation in Ancestral Rocky Mountain basins (Johnson et al., 1992; Barbeau, 2003; Soreghan et al., 2012; Sweet et al., 2021), which rendered these depocenters as recorders of the tectonic history. Updated biostratigraphic age control suggests that Ancestral Rocky Mountain basin subsidence was mostly synchronous across the orogen, initiating in the Early Pennsylvanian (ca. 318 Ma), and peaking in the Late Pennsylvanian (Sweet et al., 2021). Following this, basins to the south experienced a renewed phase of subsidence in the early Permian (ca. 285 Ma; Sweet et al., 2021).

The Central Colorado Trough developed between two major Ancestral Rocky Mountain highlands, the Uncompahgre and Apishapa uplifts, to its west and east, respectively (Figs. 1 and 2). At mid-latitudes, on the basin's western flank, the Crestone thrust fault (Fig. 2) juxtaposes Precambrian basement of the Uncompahgre Uplift against Pennsylvanian–Permian coarse-grain siliciclastic strata (Hoy and Ridgeway, 2002). In this location, stratal thickness and grain-size decrease to the east, and the Apishapa Uplift is interpreted as a potential forebulge (Hoy and Ridgeway, 2002). However, to the north, within our study area, folding of Pennsylvanian strata and development of an angular unconformity adjacent to the Apishapa Uplift (Fig. 2; De Voto and Peel, 1972; Wallace et al., 2000; Hoy and Ridgeway, 2002) suggest west-vergent faulting at depth associated with the Apishapa Uplift. The Cimarron Arch marks the southern boundary of the Central Colorado Trough and the northern boundary of the Greater Taos Trough (Fig. 2) (Baltz and Meyers, 1999; Chowdhury and Sweet, 2020). Lower Pennsylvanian strata are absent from the arch, which indicate exposure and unconformity development during this time (Baltz and Meyers, 1999). To the north, between the Central Colorado Trough and the Eagle Basin, lies the Sawatch Uplift (Fig. 2). This uplift appears to have influenced paleoflow and the depositional patterns around it but was relatively minor as it was not a notable contributor of sediment (Johnson et al., 1992).

Late Paleozoic basin history in the Central Colorado Trough spans the entirety of Ancestral Rocky Mountain activity in the region, from initial basin development to peak tectonic activity preserved in its intraformational unconformities and growth strata (De Voto and Peel, 1972; Wallace et al., 2000; Hoy and Ridgeway, 2002). Within our study area, Lower Pennsylvanian strata (Kerber and Sharpsdale formations, Fig. 3) rest on karsted Mississippian limestone (Wallace et al., 1999), which reflect fluctuations in deposition among fluvial, deltaic, and restricted carbonate shelf environments during a period of low accommodation (Peel, 1971; Musgrave, 2003). During the Middle

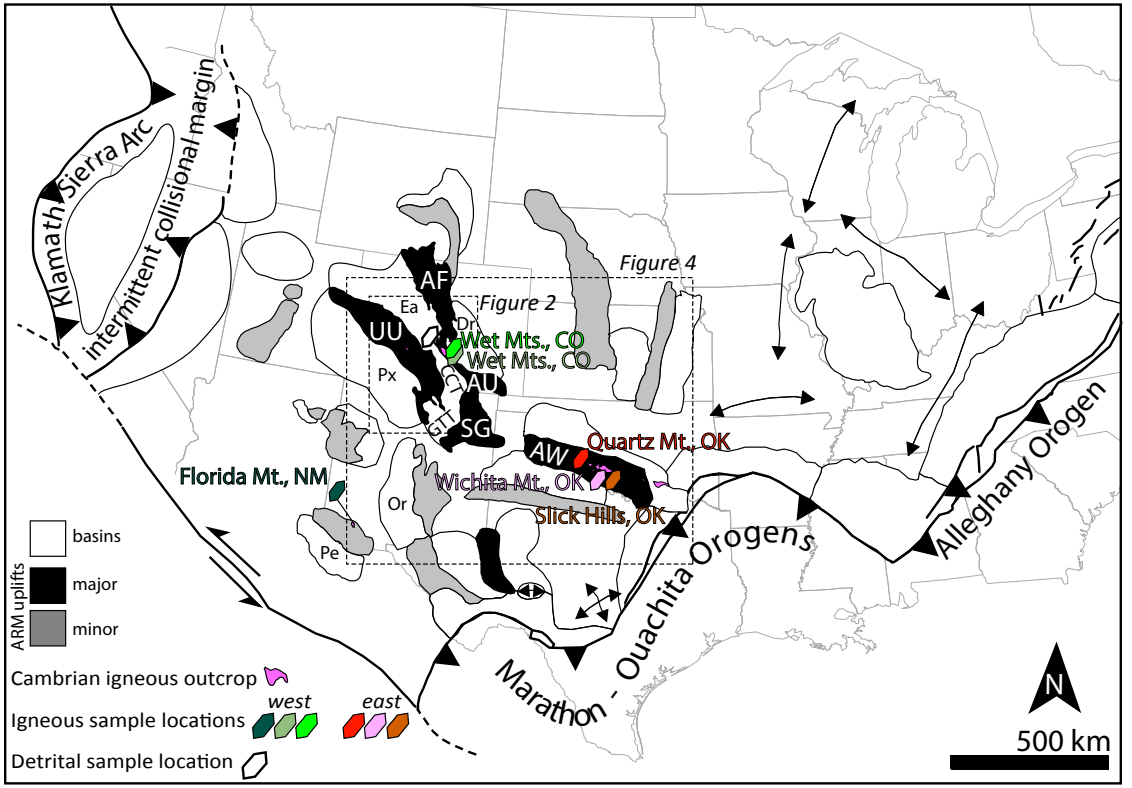

Figure 1. Map shows late Paleozoic North America with major tectonic features and the locations of salient uplifts (ARM—Ancestral Rocky Mountain, UU—Uncompahgre, SG—Sierra Grande, AU—Apishapa, AF—Ancestral Front Range, and AW—Amarillo-Wichita) and basins (EB—Eagle Basin, CCT—Central Colorado Trough, GTT—Greater Taos Trough, Px—Paradox Basin, Or—Orogrande Basin, and Pe—Pedregosa). Locations of major Cambrian igneous rock outcrops, igneous samples, and detrital sample sets are shown. Figure was adapted from Kluth and Coney (1981); Barbeau (2003); Thomas (1991); Leary et al. (2017); Lawton et al. (2017); and Sturmer et al. (2018). Shapes of the Central Colorado Trough and adjacent uplifts presented here are detailed in Figure 2, where we also provide references used in that adaptation.

Pennsylvanian, the Minturn Formation was deposited as accommodation rates increased and drove marine transgression well into the Central Colorado Trough (Musgrave, 2003; Hoy and Ridgeway, 2003; Sweet et al., 2021). During this time, both the Central Colorado Trough and Eagle Basin developed a series of fan-delta systems that deposited coarse-grain clastic sediment along basin margins and fed turbidites closer to the basin axis (Houck, 1991; Hoy and Ridgeway, 2002, 2003; Myrow et al., 2008). As the seas withdrew from the Central Colorado Trough, marine deposition, particularly along the basin axis, was replaced by proximal alluvial fan deposition (i.e., Crestone Conglomerate), which transitioned to medial fan and basin axis fluvial deposits (i.e., Sangre de Cristo Formation) in the Late Pennsylvanian–early Permian (Hoy and Ridgeway, 2002, 2003; Musgrave, 2003). The distance from basement thrust to axial fluvial deposition was only ~10 km adjacent to the Crestone thrust (Hoy and Ridgeway, 2002), which provides an approximation of alluvial fan scale in this system. The age of subaerial deposits is poorly constrained, but growth strata and near-surface fault tips document Ancestral Rocky Mountain tectonic activity in the Late Pennsylvanian–early Permian Central Colorado Trough (Hoy, 2000; Hoy and Ridgeway, 2002). During this time, an axial fluvial system flowed northward and was fed by alluvial fans along the eastern and western basin margins (Hoy and Ridgeway, 2002). The upper boundary of the Sangre de Cristo Formation is unconformably overlain by upper Permian–Lower Triassic (Freeman and Bryant, 1977) to Cenozoic strata (within our study area; Taylor et al., 1975), which provide little age control on the upper limit of deposition. The most likely period of Ancestral Rocky Mountain–related basin cessation in the Central Colorado Trough occurred in the early Permian, which is reflected in the upper age limit for the Eagle Basin to the north and the Taos Trough to the south (Sweet et al., 2021).

Cambrian Age Zircons, Geochemistry, and Rodinian Breakup

Formation of Cambrian zircon in igneous rocks throughout the midcontinent and western Laurentia was associated with the final stage of Rodinian rifting. The supercontinent of Rodinia experienced protracted break-up that

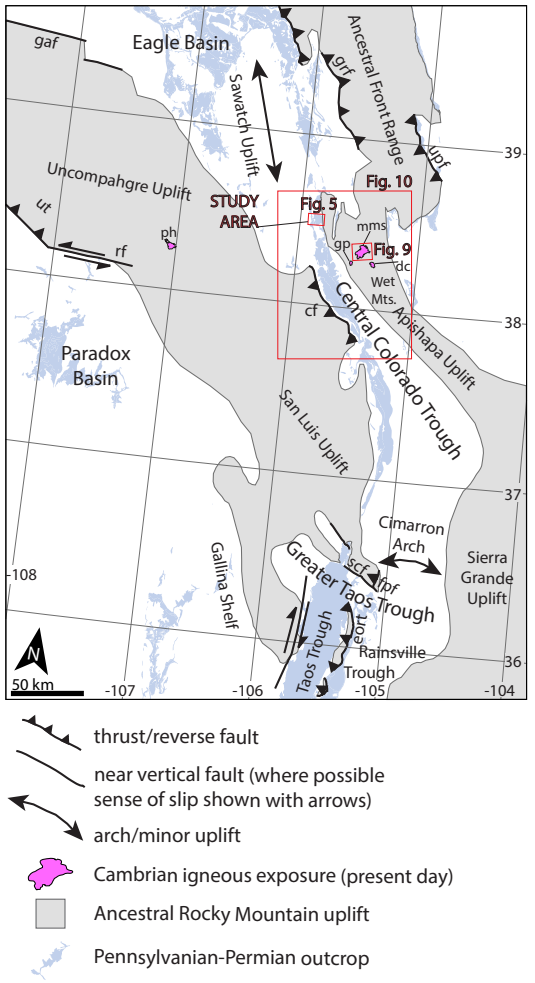

Figure 2. Map shows tectonic features around the Central Colorado Trough. Structural elements are modified from Hoy and Ridgeway (2002), De Voto et al. (1986), Woodward et al. (1999), Chowdhury and Sweet (2020), Baltz and Meyers (1999), and Sweet and Soreghan (2010). Structural features were edited according to the Colorado state geologic map (Green, 1992). There are variable degrees of uncertainty for the precise locations of uplift boundaries. Cambrian igneous bodies were modified from Olsen et al. (1977) and Green (1992). Pennsylvanian–Permian polygons are from Green (1992). Abbreviations for Cambrian intrusions: ph—Powderhorn Alkalic Complex, mms—McClure Mt. Syenite, gp—Gem Park, dc—Democrat Creek. Abbreviations for structures: cf—Crestone fault, gfz—Gore fault zone, eort—El Oro-Rincon thrust, fpf—Flower Pass fault, nf—Northern fault, ppf—Picuris-Pecos fault, rf—Ridgeway fault, scf—Saladon Creek fault, tf—Transverse fault, upf—Ute pass fault, ut—Uncompahgre thrust. In the text, the greater Taos Trough refers to the combined depocenters of the Taos Trough and Rainsville Trough (Chowdhury and Sweet, 2020).

stretched from the early Neoproterozoic to early Cambrian and occurred at different times in separate areas. The main phase of rifting along the western Laurentian margin occurred from 720 Ma to 680 Ma (Fanning and Link, 2004) and was accompanied by ≥1-km-thick rift basin development (Yonkee et al., 2014). During this time interval, the eastern margin of Laurentia experienced an episode of failed rifting (760–700 Ma; Su et al., 1994; Aleinikoff et al., 1995; Whitmeyer and Karlstrom, 2007), but then rifting successfully began at ca. 620 Ma (Whitmeyer and Karlstrom, 2007). Rifting between 650 and 530 Ma drove development of the Southern Oklahoma Aulacogen (Fig. 1; McConnell, 1988; Hanson et al., 2013), which has been interpreted as a failed rift arm (Hoffman et al., 1974) and a leaky transform boundary during rifting (Thomas, 1991). A bimodal suite of extrusive and intrusive igneous rocks in this location was emplaced here between 530 Ma and 540 Ma (Hanson et al., 2013). Approximately 300 km to the east, similar timing of rifting and associated igneous activity is proposed for the development of another major failed rift arm of the Iapetan margin (i.e., the Reelfoot Rift; Thomas et al., 2004; Freiburg et al., 2020).

West of the Southern Oklahoma Aulacogen, other Cambrian and Early Ordovician igneous rocks are present, which consist of syenites, alkali feldspar granites, carbonatites, and mafic rocks (McMillan and McLemore, 2004). These include several exposures in the areas once occupied by the Apishapa and Uncompahgre uplifts (Fig. 4). The presence of these igneous rocks, including west–northwest-striking Cambrian dikes in western Colorado and regional gravity data, have led to the interpretation of a tectono-magmatic link between the Southern Oklahoma Aulacogen and Cambrian igneous rocks in Colorado (Larson et al., 1985; Keller and Stephenson, 2007; Soreghan et al., 2012). Alternatively, slightly younger ages of igneous rocks scattered throughout the western interior of North America (574–427 Ma in Colorado, USA, and 664–457 Ma in New Mexico, USA) and their approximate north–south occurrence has led other authors (McMillan and McLemore, 2004) to hypothesize the existence of the New Mexico Aulacogen (Fig. 4), which would be the youngest failed Rodinian rift system in Laurentia.

Regardless of an association with either the Southern Oklahoma or New Mexico aulacogen, the zircon geochemistry of Cambrian igneous rocks in Colorado and New Mexico may have been affected by two emplacement conditions. (1) They were emplaced in crust west of the Nd 1.55 Ga model age line, which is interpreted to reflect a boundary between Mesoproterozoic crust to the east and Paleoproterozoic crust to the west (Fig. 4; Bickford et al., 2015); and (2) they were emplaced in a less well-developed extensional tectonic regime than rocks of similar age in Oklahoma. During Cambrian rifting, partial melting and assimilation of Proterozoic crust, which increases in age to the west, was possibly accentuated by less developed magma piping systems, and would leave distinct isotopic signatures such as low $^{176}Hf/^{177}Hf$ and $^{143}Nd/^{144}Nd$ ratios in the resultant igneous rocks. We predict a systematic east to west variation in the geochemistry of Laurentian Cambrian igneous rocks emplaced during Rodinian rifting, similar to the trend of Nd and Hf isotopic ratios observed in Mesoproterozoic granitoids across the same region (e.g., Van Schmus et al., 1993; Goodge and Vervoort, 2006; Bickford et al., 2015).

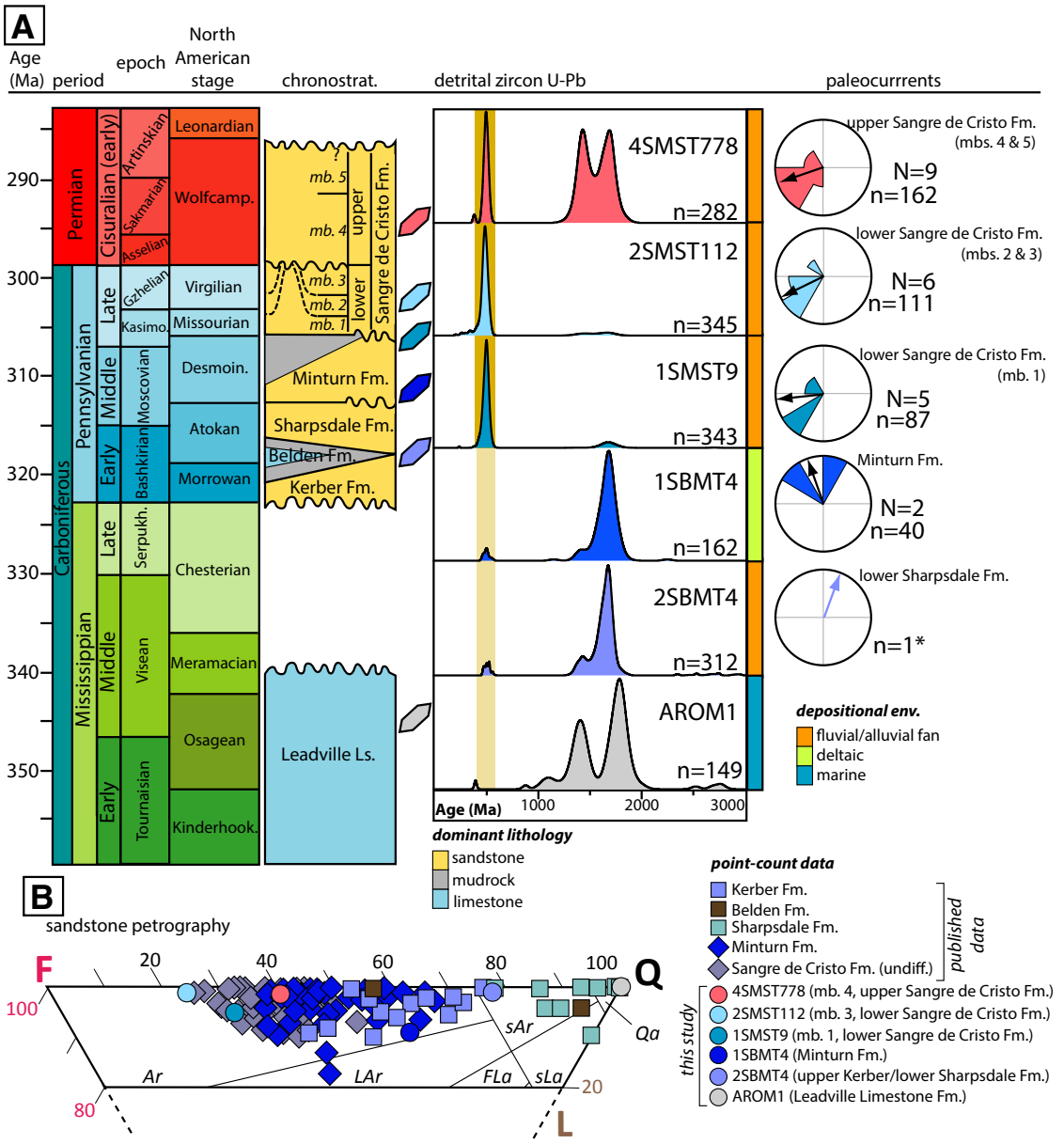

Figure 3. (A) Diagrams show chronostratigraphy, detrital zircon probability density plots (PDPs), paleocurrent data, and interpreted depositional environment of sampled units. Dashed lines in the lower Sangre de Cristo Formation (Fm.) chronostratigraphy indicate folding beneath an angular unconformity. Geologic time scale is from Artez et al. (2020) and Henderson and Shen (2020). Stratigraphy is adapted from De Voto and Peel (1972), Wallace et al. (2000), and Musgrave (2003). (B) Sandstone petrographic data were plotted on a Quartz:Feldspar:Lithics (Q:F:L) ternary diagram truncated at 20% lithics. Q:F:L diagram fields (sensu Folk, 1974): Qa—quartz arenite, sAr—subarkose, sLa—sublithic arenite, Ar—arkose, LAr—lithic arkose, Fla—feldspathic lithic arenite. Previously published point-count data for Kerber, Sharpsdale, and Belden formations are from Musgrave (2003). Previously published point-count data for Minturn and Sangre de Cristo formations are from Hoy (2000). *Indicates low-n paleocurrent, which we consider to be an estimate, rather than a station (see text for description of distinction). Mb.—member; Ls.—limestone.

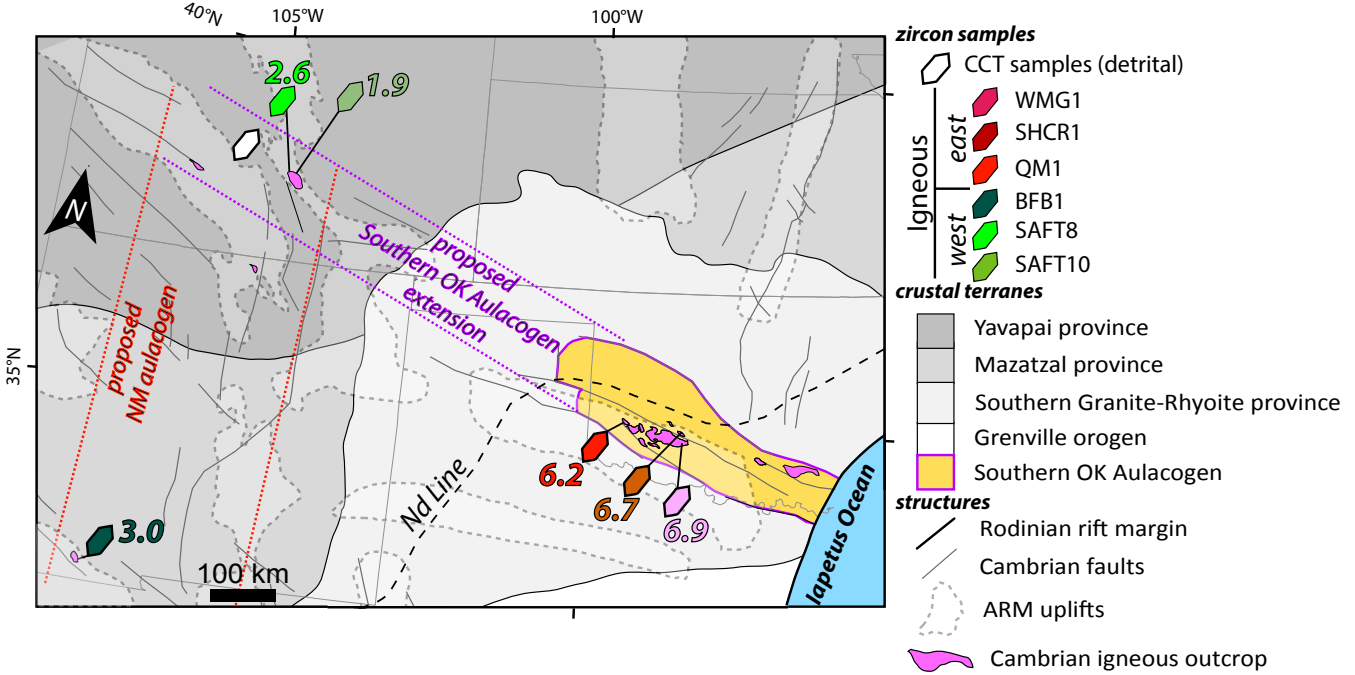

Figure 4. Laurentian crustal terrane map shows Ancestral Rocky Mountain (ARM) uplift outlines (see Fig. 1 for further information), Cambrian igneous rock exposure, sample locations, and igneous sample εHf(t) weighted mean values displayed. Proposed Southern Oklahoma (OK) Aulacogen from Larson et al. (1985) and proposed New Mexico (NM) Aulacogen from McMillan and McLemore (2004) are shown. Yavapai-Mazatzal crustal terrane boundary, faults, and rift margin are adapted from Whitmeyer and Karlstrom (2007). Southern Granite-Rhyolite province and Nd 1.55 Ga model depleted mantle age (T_{DM}) line are from Bickford et al. (2015) and references therein. ARM—Ancestral Rocky Mountains; CCT—Central Colorado Trough; NM—New Mexico; OK—Oklahoma.

While North American crustal age and geochemistry is well documented (e.g., Whitmeyer and Karlstrom, 2007; Bickford et al., 2015), there is also precedence for a predictable spatial and temporal relationship between a lower degree of rifting (i.e., less extended lithosphere) and more evolved magmatic products. East African Rift basalts exhibit a spatial pattern of more radiogenic values in isotopic ratios (i.e., $^{143}Nd/^{144}Nd$) that is associated with better-developed regions of rifting (Kampunzu and Mohr, 1991). A similar relationship is documented temporally in the southern Rio Grande Rift, though it is more complicated by preconditions set by Laramide subduction. Early rift volcanic rocks in New Mexico exhibit lower Nd isotopic ratios (i.e., $^{143}Nd/^{144}Nd$) and greater relative concentrations of incompatible to compatible trace elements (e.g., Rb/Nb and La/Nb) in comparison to younger volcanic rocks (McMillan et al., 2000). This behavior, and the advantageous assembly of older crust inboard of the failed Cambrian rifts discussed, present a scenario where geochemical tools may be useful in discerning between igneous rocks and minerals of similar ages but differing petrogenesis and locations.

METHODS

New data presented here include petrochronology of detrital and igneous zircons, thin-section description and point-counting, and paleocurrent measurement. We also include facies descriptions of sample sites in Item A in the Supplemental Material[1].

[1]Supplemental Material. Item A: Details for methods and results. Item B: Detrital zircon U-Pb data. Item C: Detrital zircon U-Pb data from REE analyses (for selected Cambrian grains). Item D: Igneous zircon U-Pb data from REE analyses. Item E: Detrital and igneous zircon REE data. Item F: Detrital and igneous zircon Hf isotope data. Item G. Paleocurrent data. Item H: Sandstone petrography data. Item I: Igneous zircon cathodoluminescence images. Please visit https://doi.org/10.1130/GEOS.S.21529104 to access the supplemental material, and contact editing@geosociety.org with any questions.

Identification of Cambrian-Age Detrital Zircons

U-Pb ages of Central Colorado Trough detrital zircons were determined via laser ablation–inductively coupled plasma–mass spectrometry (LA-ICP-MS) at the University of Houston. Individual zircon grains were mounted on double-sided tape and ablated with 240–200 shots at a 10 Hz repetition rate. Ablation spot size was 30–25 µm and conducted by a Photon Machine Analyte 193 nm ArF laser. He carrier gas introduced ablated material to a Varian 810 single-collector quadrupole LA-ICP-MS, which analyzed U, Th, and Pb isotopes. Concordant zircon grains (–10% to 20% $^{207}Pb/^{206}Pb$ versus $^{238}U/^{206}Pb$ discordance cut offs) with 2σ uncertainties that are either Cambrian or latest Ediacaran age (570–485 Ma) were selected and removed from the tape and then mounted in epoxy and polished for further analyses. Additional analytical details are provided in the supplemental data (Item A, see footnote 1).

Zircon Cathodoluminescence Imaging

Igneous zircons were mounted in epoxy and imaged using cathodoluminescence (CL) at two facilities to identify growth phases prior to Hf or REE analysis (Item I, see footnote 1). Grains were imaged using a Phillips FEI XL environmental scanning electron microscope (ESEM) equipped with a Gatan PanaCL detector at the University of Texas in Austin, Texas, USA, and a Hitachi S3400N SEM with a Gatan ChromaCL2 detector at the University of Arizona LaserChron Center, Tucson, Arizona, USA.

Zircon U-Pb and REE Analyses

In situ REE concentration measurements and U-Pb dating was performed (Table 1) over four days of analyses that occurred in 2018 and 2021 (Items A–E, see footnote 1). We included recently published U-Pb and REE data from several igneous samples (Ejembi et al., 2021), which were combined with new analyses presented here. A detailed account of which analyses are original and which were previously published is provided in Item A (Table A.1.2 in the Supplemental Material), but we also included the reduced data from those published samples in the Supplemental Material (Items D and E) for this paper in the same format as new samples for ease of navigation and replication of this work by other researchers. The REE abundances and U and Pb isotopic ratios of Cambrian-age zircons were analyzed by the same single-collector quadrupole LA-ICP-MS as described above for initial detrital analyses. Additional details of analytical procedures are provided in Item A.

Zircon U-Pb data were corrected for instrumental mass and elemental fractionations using a MATLAB-based code in UPbToolbox (Sundell, 2017; Items C and D, see footnote 1). Ages from epoxy-mounted detrital zircons were used instead of the data generated from the tape-mounted grains, and igneous grains were only analyzed in epoxy mounts. REE data were reduced, and concentrations were calculated with GLITTER software (Van Achterbergh et al., 2001). Weighted mean ages from igneous samples were calculated using IsoplotR (Vermeesch, 2018) and corrected for common Pb (Stacey and Kramers, 1975) if notable common Pb was observed in Tera-Wasserburg concordia plots (Item A). The means across the four LA-ICP-MS sessions for standards are 336.3 ± 3.6 (2 standard errors or $2\sigma_{se}$) for Plešovice ($^{238}U/^{206}Pb$), 1078.9 ± 45.0 ($2\sigma_{se}$) for FC5z ($^{206}Pb/^{207}Pb$), and 572.7 ± 7.8 ($2\sigma_{se}$) for Peixe ($^{238}U/^{206}Pb$).

TABLE 1. SAMPLE METADATA

Sample	Unit	Sample rock type	U-Pb (n)	REE (n)	εhf(t) (n)	Latitude (°N)	Longitude (°W)
WMG1	Mount Scott Granite	Granite	25	34	16	34.74601	98.53301
SHCR1	Carlton Rhyolite	Granite	22	44	21	34.82046	98.52736
QM1	Lugert Granite	Granite	28	33	16	34.88795	99.29747
BFB1	Florida Mountain Syenite	Syenite	40	57	30	32.11021	07.63753
SAFT8	McClure Mt. Syenite, nepheline	Syenite	32	40	21	38.34266	105.46259
SAFT10	McClure Mt. Syenite, hornblende-biotite	Syenite	51	51	48	38.337237	105.450915
4SMST778	Upper Sangre de Cristo Fm., mb. 4	Sandstone	282	21	21	38.48116	105.83811
2SMST112	Lower Sangre de Cristo Fm., mb. 3	Sandstone	345	28	28	38.47203	105.86271
1SMST9	Lower Sangre de Cristo Fm., mb. 1	Sandstone	343	31	31	38.47673	105.88118
1SBMT4	Minturn Fm.	Sandstone	162	2	2	38.47604	105.89128
2SBMT4	Upper Kerber/lower Sharpsdale Fm.	Sandstone	312	11	11	38.48144	105.90688
AROM1	Leadville Limestone	Sandstone	149	n/a	n/a	38.48209	105.91215

Note: Igneous and detrital metadata include unit name, rock type, number of grains used in different analyses, and location. Some analyses for some igneous samples were originally published in Ejembi et al. (2021), the details of which are provided in Item A, Table A.1.2 (see text footnote 1). REE—rare earth element; Fm.—formation; Mb.—member.

Zircon Hf-Isotopic Analyses

Hafnium isotopic compositions of zircon were measured by laser ablation using a Nu Plasma II multicollector (MC)-ICP-MS, which was equipped with a Photon Machine Excite 193 nm ArF laser with HelEx II cell at the University of Houston.

Instrumental mass fractionation (IMF) and isobaric interferences were internally corrected by calculating IMF factors for Yb and Lu based on the measured $^{179}Hf/^{177}Hf$ ratio. The zircons analyzed were relatively REE-poor, so internal IMF correction of ^{176}Yb and ^{176}Lu could not be accurately determined from the measured Yb isotopes. To test the accuracy of the method, we analyzed two zircon standards, one that is REE-poor (Plešovice; $^{176}Hf/^{177}Hf$ = 0.282482 ± 0.000013, Lu/Hf = 0.0004 – 0.0015; Sláma et al., 2008) and one that is relatively REE-rich (FC5z; $^{176}Hf/^{177}Hf$ = 0.282172 ± 0.000016, Lu/Hf = 0.001262; Woodhead and Hergt, 2005). The means of $^{176}Hf/^{177}Hf$ for the standards across the three LA-MC-ICP-MS sessions are 0.282469 ± 0.000007 ($2\sigma_{se}$) for Plešovice, and 0.282175 ± 0.000010 ($2\sigma_{se}$) for FC5z (Items A and F, see footnote 1). The ranges of Lu/Hf ratio means across these sessions are 0.00071–0.000123 for Plešovice, and 0.000653–0.000920 for FC5z (Items A and F). Hf isotopic ratios of average mantle extraction age for melt source material were calculated using the U-Pb ages from earlier analyses for respective zircon grains and $\lambda^{176}Lu$ of $1.87*10^{-5}$ /m.y. (Scherer et al., 2001; Söderlund et al., 2004). Calculated εHf(t) values utilized present-day chondrite uniform reservoir (CHUR) values of $^{176}Hf/^{177}Hf$ = 0.282785 ± 11 and $^{176}Lu/^{177}Hf$ = 0.0336 ± 1 (Bouvier et al., 2008).

Petrography and Paleocurrent Analyses

Igneous and sandstone sample thin sections were analyzed and described using a Zeiss Axio Imager.A2m polarizing binocular microscope. Framework grains in detrital samples were point-counted (n = 300) using an automatic stepping stage and Petrog3 software and were classified following Folk (1974). Sandstone thin sections from this study were cut from the same samples from which detrital zircon samples were processed. We combined our new point-count data with published counts from Musgrave (2003) and Hoy (2000).

Paleocurrent measurements were collected from a stratigraphic transect that spans the Early Pennsylvanian–early Permian and approximately parallels the Arkansas River east of Salida, Colorado, USA (Fig. 5). We selected paleocurrent measurement stations based on the presence of adequate exposure of sedimentary structures of unequivocal downstream-migrating bedforms, which in this study area were exclusively trough cross-stratified sandstones. We followed methods outlined by DeCelles et al. (1983), and they are presented in an azimuthal reference frame (Item G, see footnote 1). Paleocurrent measurement stations (N) were documented where 3-D exposure of sedimentary structures was adequate to collect ample measurements of right and left limbs (n = ~20), trough axes (n = ~10), or a combination of both. We provide a paleocurrent estimate, where we measured paleocurrent indicators, but there was an insufficient number of limbs and axes exposed to constitute a paleocurrent station.

RESULTS

Igneous Samples

Igneous samples collected in this study serve as a preliminary regional data set for petrochronologic analysis/fingerprinting of Cambrian intrusions in western and midcontinent North America. The following section presents pooled weighted-mean zircon ages with (calculated in *IsoplotR*; Vermeesch, 2018) REE patterns, and weighted-mean and median εHf(t) values. Igneous sample locations are shown in Figure 3. For more detailed information about these data, including sample descriptions and Tera-Wasserburg concordia diagrams, see Item A (footnote 1).

Eastern igneous samples (WMG1, SHCR1, and QM1) were collected from A-type felsic rocks distributed across southern Oklahoma that are part of the Southern Oklahoma Aulacogen layered bimodal suite (Hogan et al., 1995; Price, 1998; Hanson et al., 2013). These include the Wichita Mountain Granite Group (WMG1 and QM1) and the Carlton Rhyolite (SHCR1). Weighted mean sample ages from granites (WMG1, 542.8 ± 4.3 ($2\sigma_{se}$)) Ma; QM1, 532.9 ± 5.0 ($2\sigma_{se}$) Ma) fall within the broad age range reported by Powell et al. (1980; 525 ± 25 Ma). However, U-Pb zircon ages reported for the Wichita Mountain Granite (535 ± 3–530 ± 1 Ma; Wright et al., 1996; Degeller et al., 1996; Hanson and Eschberger, 2014) are younger than WMG1's weighted mean age and standard error but are within its standard deviation (Item A, footnote 1). Conversely, WMG1's age fits within the age range reported for amphibole $^{40}Ar/^{39}Ar$ (539 ± 2) from the same granite (Hames et al., 1998). The weighted mean zircon age from the Carlton Rhyolite (SHCR1, 533.8 ± 4.1 ($2\sigma_{se}$) Ma) is consistent with published U-Pb zircon ages from this unit (539 ± 5 Ma and 536 ± 5 Ma; Thomas et al., 2012). Almost all zircons exhibit REE patterns with high heavy REE (HREE) to light REE (LREE) ratios, negative Eu anomalies, and positive Ce anomalies (Figs. 6A and 6C). Analyses not containing Ce anomalies commonly exhibit higher LREE to HREE ratios than those that do. Weighted mean εHf(t) values for eastern samples are 3–5 ε-units higher (WMG1, 6.9; SHCR1, 6.7; QM1, 6.2) than those of western samples (BFB1, 3.0; SAFT8, 2.6; SAFT10, 1.9) (Fig. 6; Table 2; Item A).

Western igneous samples were collected from syenites in southern New Mexico (BFB1) and central Colorado (SAFT8 and SAFT10; Fig. 4). The weighted mean age of sample BFB1 (509.0 ± 3.6 ($2\sigma_{se}$) Ma), which was collected from the Florida Mountains Syenite, is consistent with previously published ages (503 ± 10 Ma and 514 ± 3 Ma; McMillan and McLemore, 2004). In central Colorado, Wet Mountains samples (SAFT8 and SAFT10) are from the McClure Mountain alkaline-mafic suite (Olson et al., 1977). SAFT8 is a nepheline syenite, and SAFT10 is a biotite-hornblende syenite. While Wet Mountains sample ages are consistent with one another (SAFT8, 533.3 ± 3.7 ($2\sigma_{se}$) Ma; SAFT10, 532.1

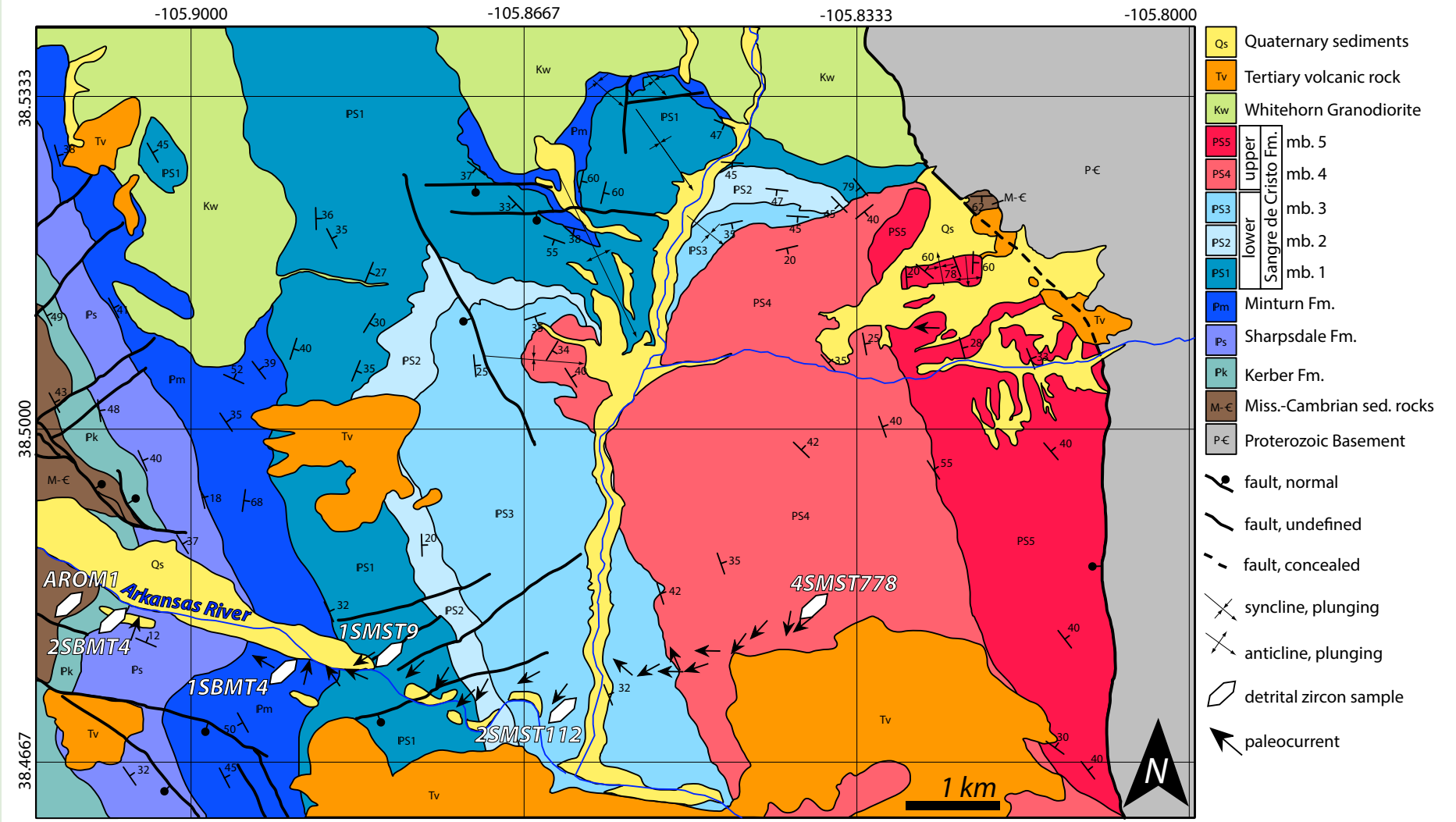

Figure 5. Geologic map of Arkansas River Valley shows detrital zircon sample and paleocurrent locations. Several geologic maps were used to make this map (De Voto and Pierce, 1971; Tayler et al., 1975; Wallace et al., 1997, 2000). Although much consistency exists across these reference maps, the respective authors differ in some formation distinctions. By combining these maps to cover the area of interest, we were required to extrapolate formation contacts in areas that were not mapped. Fm.—formation; Mb.—member.

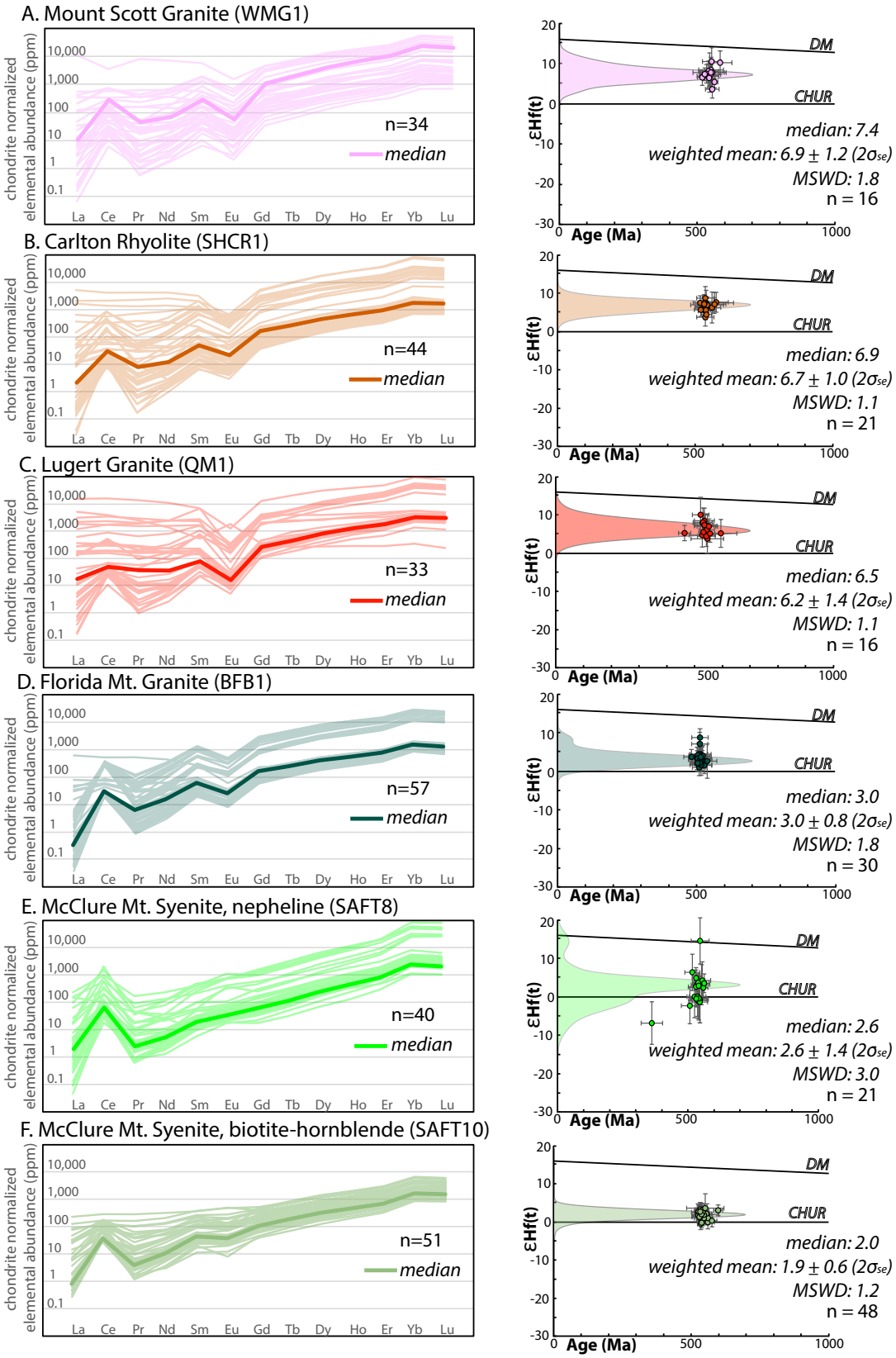

Figure 6. Chondrite-normalized rare earth element and εHf(t) value plots of igneous samples are shown. εHf(t) data points show 2σ uncertainty bars for U-Pb age and εHf(t). εHf(t) plots also show probability density plots in e-space displayed behind data points. Mean squared weighted deviations (MSWDs) are in reference to the εHf(t) weighted means for each sample, which are presented with 2 standard error ($2\sigma_{se}$). Some analyses in samples WMG1, QM1, SHRC1, BFB1, and SAFT8 are from Ejembi et al. (2021). See Table A.1.2. in Item A (see text footnote 1) for details about which analyses are new and which were previously published. DM—depleted mantle; CHUR—chondritic uniform reservoir.

TABLE 2. SAMPLE εHf(t) T-TESTS

		Basin samples					Cambrian sources					
		2SBMT4	1SBMT4	1SMST9	2SMST112	4SMST778	SAFT8	SAFT10	BFB1	QM1	SHCR1	WMG1
Basin samples	2SBMT4	1.00	0.66	0.09	0. 01	0.05	0.79	0.66	0.08	0.00	0.00	0.00
	1SBMT4	0.66	1.00	0.39	0.20	0.34	0.59	0.59	0.41	0.20	0.20	0.17
	1SMST9	0.09	0.39	1.00	0.08	0.62	0.24	0.03	0.85	0.00	0.00	0.00
	2SMST112	0.01	0.20	0.08	1.00	0.18	0.02	0.00	0.05	0.31	0.18	0.06
	4SMST778	0.05	0.34	0.62	0.18	1.00	0.14	0.02	0.45	0.00	0.00	0.00
Cambrian sources	SAFT8	0.79	0.59	0.24	0.02	0.14	1.00	0.98	0.24	0.00	0.00	0.00
	SAFT10	0.66	0.59	0.03	0.00	0.02	0.98	1.00	0.00	0.00	0.00	0.00
	BFB1	0.08	0.41	0.85	0.05	0.45	0.24	0.00	1.00	0.00	0.00	0.00
	QM1	0.00	0.20	0.00	0.31	0.00	0.00	0.00	0.00	1.00	0.53	0.11
	SHCR1	0.00	0.20	0.00	0.18	0.00	0.00	0.00	0.00	0.53	1.00	0.18
	WMG1	0.00	0.17	0.00	0.06	0.00	0.00	0.00	0.00	0.11	0.18	1.00

Note: T-test p-value table of detrital and igneous (i.e., possible Cambrian sources) sample εHf(t) values. Colors provide an auxilary measure of p-values, green to red, indicating high to low, respectively.

± 2.1 ($2\sigma_{se}$) Ma), they are older than the reported age of the biotite-hornblende syenite (523.98 ± 0.12 Ma; Schoene and Bowring, 2006). However, the standard deviation of both ages overlaps with the Schoene and Bowring age (Item A, footnote 1). Furthermore, the SAFT8 and SAFT10 samples were collected from outcrops separate from where the Schoene and Bowring (2006) sample was collected (the quarry-derived parking lot boulder; Alexander et al., 1978), and therefore they are likely from different parts of the Wet Mountains intrusive complex. BFB1 REE patterns are like those described for eastern samples, whereas all SAFT8 analyses uniquely exhibit no negative Eu anomaly (Figs. 6D and 6E). SAFT10 zircons exhibit both the presence and absence of negative Eu anomalies, display high HREE:LREE ratios, and most have a positive Ce anomaly (Fig. 6F).

Detrital Samples

Detrital samples were collected along a contiguous outcrop of late Paleozoic strata, which ensures a robust relative chronology (Fig. 5). Zircon REE and εHf(t) data are presented similar to igneous data (Fig. 6) in Figure 7. Age assignment of units is primarily from Wallace et al. (1997, 2000), except for Lower Pennsylvanian strata (i.e., Kerber and Sharpsdale formations), where we defer to age assignments from Musgrave (2003) because of his more detailed and recent biostratigraphic analyses. The following section presents an overview of detrital zircon age distributions (Fig. 3A), and REE and εHf(t) data for Cambrian zircons (Fig. 7), along with sandstone petrography, paleocurrent data (Fig. 3B), and a brief description of lithofacies. For a more detailed treatment of these data, as well as data tables, see Items A–C and E–H (footnote 1).

Mississippian–early Permian Central Colorado Trough samples, paleocurrent measurements, and descriptive data were collected in a contiguous section along the Arkansas River in central Colorado (Fig. 5). The farthest west and oldest sample (AROM1) was collected from an ~1-m-thick, lenticular sandstone within the Leadville Limestone. At this location, the limestone is a black-gray micrite, which contains sparse fossils, occasional beds composed of micritic intraclasts, and centimeter-scale, discontinuous lenses of siltstone to very fine-grained sandstone. The sandstone is a muddy (>30% silt matrix) quartz sandstone (quartz: feldspar: lithic or Q:F:L of 98:2:0; Fig. 3B), with rounded framework grains, silty matrix, and microcrystalline calcite cement (Fig. 8L). Detrital zircon age spectra contain no Cambrian zircons and exhibit two subequal dominant modes at 1.79 Ga and 1.41 Ga, a 1.12 Ga shoulder, a few single age peaks from the late Paleozoic (ca. 400 Ma) to the Neoproterozoic (ca. 600 Ma), and two minor Archean age modes (Fig. 3A).

Data for Lower and Middle Pennsylvanian strata include samples, measurements, and descriptions of the approximate Kerber/Sharpsdale Formation contact (2SMBT4) and the Minturn Formation (1SMBT4). Sample 2SMBT4 was collected from a fine- to coarse-grained, trough cross-stratified sandstone, interbedded with silty red mudstones that exhibit pervasive blocky fractures. Sample 1SMBT4 was collected from a concave-up–shaped, medium- to coarse-grained, cross-stratified sandstone interbedded with massive red silty mudstone and dark fissile, clay-rich mudstone. Sandstone composition between these two samples exhibits a an upsection trend of increasing feldspar

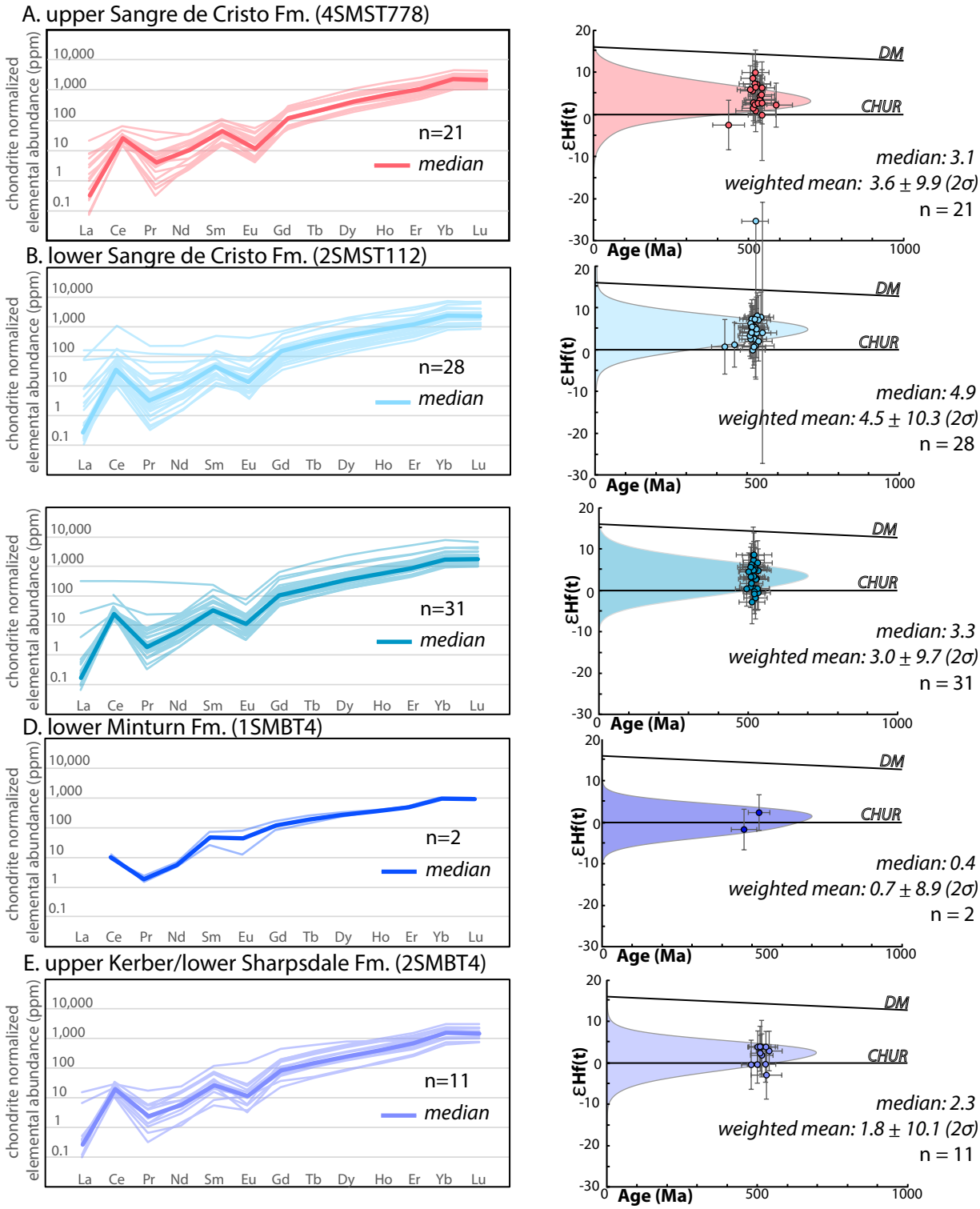

Figure 7. Chondrite-normalized rare earth element and εHf(t) value plots of Cambrian zircons from detrital samples are shown. εHf(t) data points show 2σ uncertainty bars for U-Pb age and εHf(t) data. εHf(t) plots also show probable density plot in e-space displayed behind data points, and weighted means are presented with 2σ uncertainty bars. DM—depleted mantle; CHUR—chondritic uniform reservoir; Fm.—formation.

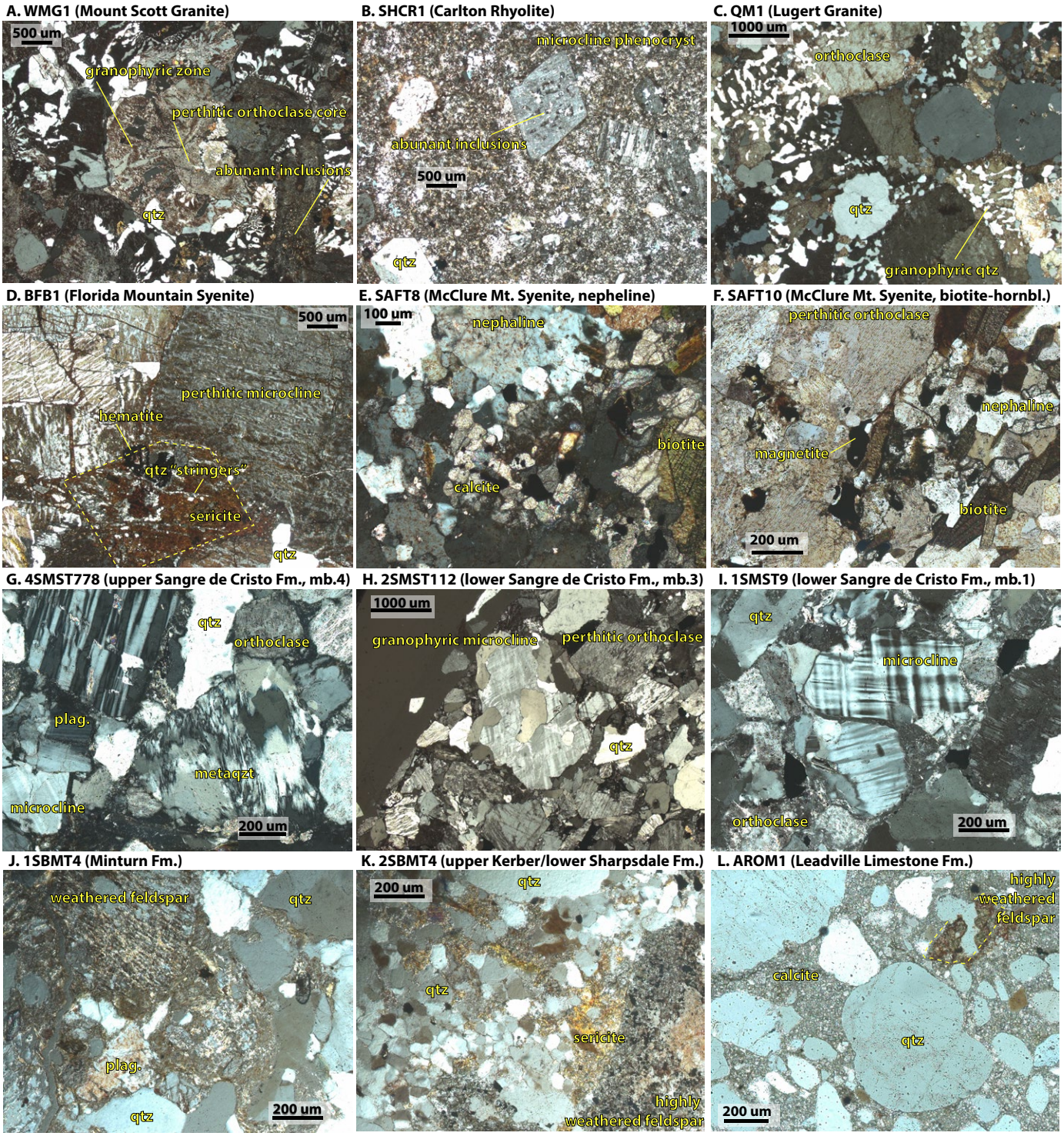

Figure 8. Photomicrographs of igneous and detrital samples are shown. (A) WMG1 shows pervasive granophyric texture surrounding a perthitic orthoclase core. The photomicrograph also shows abundant inclusions in orthoclase crystal. (B) SHCR1 shows microcline and plagioclase phenocrysts, some of which have abundant inclusions. Image also shows euhedral quartz (qtz) phenocryst. (C) QM1 shows abundant granophyric texture, orthoclase, and mono-crystalline quartz. (D) BFB1 shows large alkali feldspars with pervasive perthitic texture and minor quartz. Image also shows abundant sericite with internal zones of polycrystalline quartz, some of which form linear features (a.k.a. stringers). This zone may be thoroughly altered grain (dashed yellow outline; feldspar?) with the quartz stringers preserving relict grain structure. (E) SAFT8 shows nepheline feldspathoid (dusty in appearance), magnetite, and calcite in association with biotite. (F) SAFT10 shows large perthitic orthoclase crystals and a finer-grained cluster of nepheline (dusty in appearance), orthoclase or untwinned plagioclase, biotite, and magnetite. hornbl.—hornblende. (G) 4SMST778 shows abundant feldspar grains, including microcline, orthoclase, and plagioclase. Image also shows a polycrystalline quartz grain that exhibits metamorphic texture. (H) 2SMST112 shows dominantly arkosic composition with perthitic orthoclase and a granophyric textured microcline grain. (I) 1SMST9 shows dominantly arkosic composition with orthoclase and microcline grains. (J) 1SBMT4 shows monocrystalline quartz and variable weathering of feldspar grains. plag.—plagioclase. (K) 2SBMT4 shows bimodal grain-size distribution with the smaller fraction dominated by quartz. Image also shows two large, highly weathered feldspar grains. (L) AROM1 shows rounded, poorly sorted quartz grains in a calcite matrix. Note the highly weathered feldspar grain with granophyric quartz. Fm.—formation; mb.—member.

abundance (77:22:1–59:32:9; Fig. 3B). Musgrave (2003) noted a similar upsection trend of increasing feldspar content from the Kerber Formation (mean 95:4:1, N = 16) to the Sharpsdale Formation (mean 62:34:4, N = 14; Fig. 3B). The latter is consistent with our Kerber/Sharpsdale Formation contact sample (2SMBT4). Paleocurrent measurements indicate northward sediment transport (Fig. 3A) and are consistent with regional data (De Voto and Peel, 1972; Waechter and De Voto, 1989; Hoy and Ridgeway, 2002). Detrital zircon age spectra for both samples are similar and contain a dominant mode at 1.67 Ga, a shoulder at 1.43 Ga, and a minor age distribution between 460 Ma and 580 Ma (Fig. 3A). Cambrian-age detrital zircons from both samples also exhibit similar low εHf(t) weighted means (2SMBT4, 1.8; 1SMBT4, 0.7), and REE trends with increasing HREE:LREE abundances, most of which contain negative Eu anomalies (Figs. 7D and 7E). Cambrian zircon weighted mean εHf(t) values for Lower–Middle Pennsylvanian strata (2SMBT4, 1.8; 1SMBT4, 0.9) are 1–3 ε-units lower than those of detrital zircons of similar age in Upper Pennsylvanian–lower Permian samples (1SMST9, 3.0; 2SMST112, 4.5; 4SMST778, 3.6; Figs. 7A–7C; Item A).

The Upper Pennsylvanian and lower Permian strata sampled and paleocurrents described here are from members 1 (1SMST9) and 3 (2SMST112) of the lower Sangre de Cristo Formation and member 4 (4SMST778) of the upper Sangre de Cristo Formation (Wallace et al., 1997, 2000). In our study area, the boundary between the Minturn and Sangre de Cristo formations is a thin (<1 m) gypsum bed within a package of black shale (Taylor et al., 1975), but this contact can be unconformable in other locations (De Voto and Pierce, 1971; De Voto, 1980). The Sangre de Cristo Formation in this area is predominantly a medium- to coarse-grained, poorly sorted, arkosic sandstone, interbedded with red silty mudstone, and contains an angular unconformity between the upper and lower members (Figs. 2 and 7; Pierce, 1969; De Voto et al., 1971; Taylor et al., 1975; Wallace et al., 2000). The lower Sangre de Cristo Formation samples continue the trend of increasing feldspar content upsection (30:64:6–24:75:1), whereas the upper sample (4SMST778) marks a decrease in feldspar and corresponding increase in quartz (40:59:1; Fig. 3B). Quartz grains are almost entirely monocrystalline, but a slight increase (from 1% to 4%) in polycrystalline quartz is noted in the upper member (4SMST778). Paleocurrent data indicate a consistent west–southwest sediment transport direction throughout the formation, but their distribution becomes broader in the upper unit (Fig. 3A). It is important to note that our paleocurrent observations are different than those documented by previous research (De Voto and Peel, 1972; Hoy and Ridgeway, 2002). We use our paleocurrent measurements within the confines of our study area and defer to previous work outside of the study area; the rationale for this treatment of data is provided in the discussion section. The lower Sangre de Cristo Formation detrital zircon age spectra are defined by unimodal Cambrian age distributions (peaks at ca. 494 Ma and ca. 510 Ma; Fig. 3A). Age spectra from the upper member contain a prominent Cambrian mode (ca. 505 Ma), but its dominance is supplanted by a bimodal Proterozoic distribution (1.43 Ga and 1.69 Ga). Almost all Cambrian zircon REE patterns exhibit increased HREE to LREE abundances, negative Eu anomalies, and positive Ce anomalies (Figs. 7C–7E).

DISCUSSION

The Challenge of Age Assignments

The detrital data set presented here benefits from being collected within a well-exposed, contiguous stratigraphic section (Fig. 5), albeit one that contains unconformities (Fig. 3), which provides a robust relative chronology despite uncertainty in absolute chronology. Ages for Paleozoic strata in the Central Colorado Trough are uncalibrated relative ages that are based primarily on fusilinid and conodont biostratigraphy in marine intervals of the Kerber, Sharpsdale, and Minturn formations (Brill, 1952; Lindsey et al., 1986; Musgrave, 2003). Sangre de Cristo Formation age control is based on Missourian age vertebrate fossils found in the lower part of the formation within our study area (Vaughn, 1972). Data outside of our study area indicate that the Sangre de Cristo Formation ranges from Atokan–Desmoinesian (south of our study area in the Central Colorado Trough; Lindsey et al., 1986) to Wolfcampian (farther south in the Taos Trough; Baltz and O'Neill, 1980). In consideration of these data, we present our best estimate of age, acknowledge the uncertainty of age assignment in these rocks, and leverage the continuity of the exposed section from which the new data we present were collected.

Sediment Sources of the Northern Central Colorado Trough

A sharp change in detrital zircon age spectra from the Minturn Formation to the lower Sangre de Cristo Formation, from a dominant 1.67 Ga mode and a minor 1.43 Ga age mode to a Cambrian unimode (Fig. 3A), marks a drastic shift in sediment source. Subsequent reintroduction of similar Paleoproterozoic and Mesoproterozoic detrital zircon modal ages (1.69 Ga and 1.43 Ga) in the upper Sangre Cristo Formation mark another change in catchment and tectonic activity in adjacent uplift(s) and the basin. We endeavor to describe these Paleozoic sediment sources through the integration of source and sink zircon petrochronology, additional provenance proxies, and contextual geologic data.

Prior to Ancestral Rocky Mountain basin development, the area of the future Central Colorado Trough was a shallow seaway in the Early–Middle Mississippian that resided on the northern flank of the transcontinental arch, and it was dominated by carbonate deposition (Soule, 1992; Armstrong et al., 1992). Siliciclastic input to our study area was minor and composed of silt-rich quartz sand (Fig. 8L) that was deposited in the form of small channels (~1 m) or thin sheets (centimeter-scale) within a carbonate mud-dominated environment. Detrital zircon modes observed in these sandstones (Fig. 3A) with ages of 1.79 Ga, 1.41 Ga, and the minor 1.12 Ga are common Laurentian basement ages of Yavapai, Mesoproterozoic granitoids, and Grenville, respectively (Whitmeyer and Karlstrom, 2007). The latter age could also be contributed by exposure of the Pikes Peak Batholith (Guitreau et al., 2016) tens of kilometers to the east of the Central Colorado Trough, which was indeed exposed during the Pennsylvanian and supplied zircons of this age to the Denver Basin (Leary et al.,

2020). In combination with minor zircon ages of the Paleozoic, Neoproterozoic, and Archean, we interpret this pre-Ancestral Rocky Mountain multi-modal sediment source to reflect contribution, mixing, and recycling from a large area in western Laurentia and perhaps beyond.

Marking early Ancestral Rocky Mountain development, Early–Middle Pennsylvanian Central Colorado Trough detrital zircons within our study area exhibit Paleoproterozoic (ca. 1.67 Ga) and Mesoproterozoic (ca. 1.43 Ga) ages, which have possible basement and sedimentary sources, and indicate a constriction of source area. The former age is associated with the Mazatzal crustal terrane and intrusions (Whitmeyer and Karlstrom, 2007), and the latter is found in granitoids scattered across the midcontinent and western Laurentia (Whitmeyer and Karlstrom, 2007; Bickford et al., 2015). These ages are also found in late Neoproterozoic and early Paleozoic strata throughout western Laurentia (Matthews et al., 2018). The minor mode of Cambrian zircon in the Kerber/Sharpsdale and Minturn formations exhibits εHf(t) that closely matches zircon εHf(t) of the Wet Mountains (Figs. 6E, 6F, and 7E; Table 2). These zircons also display a mix of REE patterns; most but not all have negative Eu anomalies (Figs. 7E and 7F), as do the igneous zircons of the Wet Mountains (specifically sample SAFT10; Fig. 7F). However, while these zircons may have been originally sourced by the Wet Mountains, or by Wet Mountains-like Cambrian intrusions, higher quartz content, which decreased from Kerber to Minturn deposition (Fig. 3B; Musgrave, 2003), supports the presence and diminishing contribution of one or more recycled source. Finally, north-directed paleocurrent data (Fig. 3A) indicate a sediment source for Early–Middle Pennsylvanian strata that is to the south–southwest of the Central Colorado Trough (De Voto and Peel, 1972; Hoy and Ridgeway, 2002). This drainage model is consistent with both a direct-from-basement source, either in the Wet Mountains or Uncompahgre highlands, or a recycled sedimentary source that received zircon from those basement exposures during its deposition. In summary, the source area of the Early–Middle Pennsylvanian northern Central Colorado Trough was to the south–southwest of the depocenter, contained at least some sedimentary rocks that were unroofed throughout this period, and contributed mostly Paleoproterozoic, lesser Mesoproterozoic, and minor amounts of Cambrian zircon.

The overlying Sangre de Cristo Formation is composed of medium- to coarse-grained, arkosic sandstone that was deposited in fluvial environments (Lindsey et al., 1986; Hoy and Ridgeway, 2002) and exhibits a dramatic shift in detrital zircon spectra and a westward rotation in paleocurrent (Fig. 3) within our study area. De Voto and Peel (1972) and Hoy and Ridgeway (2002) report north–northeastward paleocurrent data in our study area, which are inconsistent with our observations in the Sangre de Cristo Formation. Contextual data for their measurements (i.e., sedimentary structure and method of measurement) are sparse in these sources, albeit Hoy and Ridgeway (2002) providing notably more than De Voto and Peel (1972), and we are not confident that many of these measurements were taken on definitively downstream-migrating structures (e.g., trough cross-stratification). Additionally, there is a greater abundance of potassium feldspar within our study area in comparison to fluvial deposits of similar age to the south (Hoy, 2000). This indicates that the proposed up-dip axial fluvial system to the south (Hoy and Ridgeway, 2002) was, at a minimum, not the only source of sediment in our study area (Hoy, 2000), and it may not have contributed any sediment to the Sangre de Cristo Formation of our study area. All of the provenance data presented here, insights from detrital zircon data discussed below, and the syndepositional development of highlands directly to the east of our study area (Hoy and Ridgeway, 2002) support a model of westward (transverse) rather than northward (axial) sediment transport through our study area during deposition of the Sangre de Cristo Formation.

The shift to simple Cambrian zircon spectra and high feldspar content in the Sangre de Cristo Formation point to a further constriction of source area defined by proximal basement exposure and limited catchment rock type (i.e., adjacent Ancestral Rocky Mountain uplift). These features are characteristic in the proximal to medial reaches of many Ancestral Rocky Mountain basins (Leary et al., 2020). The Denver Basin, which is on the other (eastern) side of the Apishapa and Ancestral Front Range uplifts (Fig. 2), contains sandstones of similar lithofacies, composition, and age, which have east-directed paleocurrents (Sweet and Soreghan, 2010), all of which support exhumation of the intervening highland during Sangre de Cristo deposition. The associated topography and drainage divide would have also blocked the Central Colorado Trough from sediment sources east of those uplifts (e.g., Amarillo-Wichita Uplift; Figs. 1 and 2). Similarly, evidence for the Uncompahgre Uplift to the west (Lindsey et al., 1986; Hoy and Ridgeway, 2002; Blakey, 2009) and the Cimarron Arch to the south (Baltz and Meyers, 1999) would have effectively isolated the Central Colorado Trough from outside of these bounding Ancestral Rocky Mountain uplifts. However, this source isolation primarily pertains to sediment transported by water, and evidence of a cosmopolitan mixture of detrital zircon sources from around Laurentia is found in the Permian loessite deposits of the Eagle Basin (Soreghan et al., 2014), which demonstrates this important caveat.

Sangre de Cristo Formation detrital zircon data point to a proximal, newly exhumed sediment source that tapped Cambrian igneous rock to the east of the study area. The unimodal Cambrian age peak of the lower Sangre de Cristo Formation (Fig. 3A) demonstrates its monolithic catchment lithology and unadulterated sediment transport signal. Cambrian igneous rocks, unlike their Proterozoic counterparts, have limited volume and constitute little of the North American basement (McMillan and McLemore, 2004; Whitmeyer and Karlstrom, 2007). While not as well correlated as Lower–Middle Pennsylvanian strata, Sangre de Cristo Formation zircon εHf(t) values, in aggregate, more closely match western igneous sources than eastern igneous sources (Figs. 4, 6, and 7). The one exception is the lower Sangre de Cristo Formation sample 2SMST112, which exhibits an elevated modal distribution and weighted mean. T-test p-values indicate a low probability (<0.05) that 2SMST112 εHf(t) values were drawn from either SAFT10 or SAFT8 source areas (Table 2). Nevertheless, the range of εHf(t) values from 2SMST112 overlaps that of both SAFT10 and SAFT8. Furthermore, other provenance proxies (e.g., zircon REE, paleocurrent, and sandstone composition) are consistent with samples from

strata above and below 2SMST112, which suggests that the sediment source did not drastically change during this interval. We interpret the elevated εHf(t) values in 2SMST112 zircons to reflect the variability of Cambrian igneous intrusive systems in western Laurentia and suggest a source of detritus during Ancestral Rocky Mountain deformation associated with, but different from, the Wet Mountains area. Most samples from the Sangre de Cristo Formation display definitive negative Eu anomalies, with only a few exhibiting muted anomalies (Figs. 7A–7C). Moreover, the abundance of microcline in Sangre de Cristo Formation samples (Figs. 8G–8I) and its relative scarcity in the McClure Mountain Syenite (Figs. 8E and 8F), as well as likely low zircon fertility of this low-silica igneous rock, support a sediment source different than the present-day exposure in the Wet Mountains. In summary, Sangre de Cristo Formation provenance data support a source model of limited catchment size, proximal basement, and containing Cambrian zircons, which exhibit εHf(t) and U-Pb ages similar to those of the Wet Mountains but of a different rock type (based on high feldspar content and zircon REE; Belousova et al., 2002) and in a different location (based on westward paleocurrent data).

This Cambrian basement appears to be the only source during deposition of the lower Sangre de Cristo Formation, but it constitutes a portion of the source area during deposition of the upper member (Fig. 3A). The presence of an angular unconformity at the base of the upper member (De Voto and Peel, 1972; Wallace et al., 2000; Hoy and Ridgeway, 2002) denotes syndepositional tectonic activity and the removal of some lower member strata. It is possible that some degree of internal catchment recycling occurred during this time, the interpretation of which is supported by lower feldspar and higher quartz abundance in the upper Sangre de Cristo Formation (Fig. 3B). Detrital zircon data indicate that the once-dominant Cambrian source was supplanted by Paleoproterozoic and Mesoproterozoic ages that are common in the Yavapai crustal terrane on which the basin is floored and of which uplifts are comprised (Whitmeyer and Karlstrom, 2007). Continued westward sediment transport, indicated by paleocurrent data, and the presence of fault propagation basement folds within our study area, adjacent to the Apishapa Uplift (Hoy and Ridgeway, 2002, their fig. 14B), support a model of continued deformation directly before and possibly during upper Sangre de Cristo deposition.

Laurentian Cambrian Zircons and Zircon Petrochronology

This study demonstrates the utility of an approach to provenance analysis that integrates source and sink zircon petrochronology to reconstruct ancient source areas. It also highlights the level of detail gleaned from such a study. Igneous data presented here show an east-to-west decrease of 3–5 εHf(t) units in Cambrian zircons from the midcontinent to western North America, yielding a tool to discriminate between eastern and western zircon sources. Zircon REE composition can be useful when matching the specific rock type to the detrital zircon (Belousova et al., 2002). However, it can be misleading in cases where the source of the igneous complex contains multiple rock types that exhibit differing REE ratios but are not all characterized. This type of REE compositional variability is demonstrated between the two Wet Mountains syenite samples presented here (SAFT8 and SAFT10), which were collected from two different syenite intrusions within the same igneous complex (Fig. 9). In this case, we interpret the absence of a negative Eu in zircons to reflect the variability in mineralogy of Cambrian igneous rock type exposed in the Wet Mountains of the Apishapa Uplift. We attribute the lack of a negative Eu anomaly in the nepheline syenite (SAFT8) to a dearth of plagioclase in that rock (Fig. 8E). Plagioclase crystallizes before zircon and has an affinity for Eu in its 2^+ valence state relative to other REEs (Sun et al., 2017). Therefore, the trace abundance of plagioclase in the nepheline syenite is consistent with the absence of a negative Eu anomaly. However, the adjacent biotite-hornblende

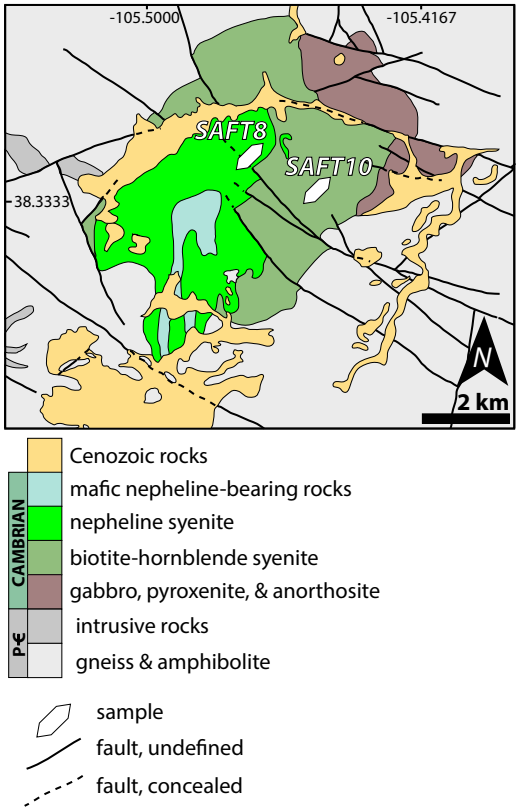

Figure 9. Geologic map of the McClure Mountain Syenite (adapted from Olsen et al., 1977) in the Wet Mountains shows SAFT8 and SAFT10 sample locations. Location of map is shown in Figure 2.

syenite (SAFT10) contains plagioclase (Fig. 8F) and mostly yields zircons with REE patterns that are depleted in Eu (Fig. 7F).

Using zircon petrochronology, paleocurrent, and petrographic data, we propose the presence of a Cambrian-aged igneous intrusion that is tectonomagmatically related to slightly older igneous rocks in the Wet Mountains; it bears zircons of similar εHf(t) but different rock type. This hypothesized Cambrian igneous rock was mostly, if not fully, eroded away. Any possible remnants would be mantled by Cenozoic volcanic rock to the northeast of the study area. However, although this rock does not outcrop in the present day, its record resides in the detritus of the Sangre de Cristo Formation. Based solely on the detrital record, this Cambrian igneous body was likely a microcline-rich granitoid with an Hf-isotopic ratio like that of other western Cambrian intrusions, but slightly younger (ca. 490–510 Ma) than the Wet Mountains intrusions to the south. Furthermore, scattered remnants of early Paleozoic rock preserved on basement to the east of the study area constrain the scale of the igneous body and suggest that the intrusion was likely small, less than or equal to tens of square kilometers, and within ~5–15 km of the basin.

Linking unimodal Cambrian zircon age distributions in the Sangre de Cristo Formation to proximal sediment sources in Colorado has implications for regional paleogeographic reconstructions. Moreover, we demonstrate that it is unnecessary to invoke distal sources of Cambrian zircons (e.g., Amarillo-Wichita Uplift; Fig. 1) for sedimentary rocks in western Laurentia that may be separated by significant drainage divides during deposition. For example, Dickinson et al. (2010) interpreted Cambrian-age detrital zircons in the Triassic Gartra Formation to have been delivered by a paleo–Eagle River that threaded its way between two remnant Ancestral Rocky Mountain uplifts, transporting sediment from southern Oklahoma to northeastern Utah (see their fig. 1). The results of this research suggest that Cambrian zircons in Triassic strata of Utah may not be derived from southern Oklahoma. Rather, sediment could have originated in proximal igneous or sedimentary sources in Colorado or New Mexico. Furthermore, our results indicate that this proximal versus distal Cambrian detrital zircon source hypothesis for the Triassic strata in Utah (and other areas) can be tested with analysis of detrital zircon εHf(t).

Tectonic Activity and Drainage Reorganization in the Northern Central Colorado Trough

Using the data and interpretations discussed above, we describe three stages of Early Pennsylvanian–early Permian tectonic activity and attendant shifts in sediment routing in the Central Colorado Trough. We focus particularly on the northern end of the basin, around the study area, but also tie these interpretations to published data throughout the depocenter to provide greater geologic context. The Kerber, Sharpsdale, and Minturn formations constitute Stage 1, which starts with Early Pennsylvanian Central Colorado Trough initiation (Leary et al., 2020) as early Ancestral Rocky Mountain–related sediments are deposited on top of the karsted Leadville Limestone. Sediments deposited during this stage record the unroofing (Musgrave, 2003) of local uplift(s) by an evolving compositional trend from quartz-rich to arkosic sandstone throughout the Early–Middle Pennsylvanian (Figs. 3B and 10). Coeval unroofing in the Denver Basin is documented by clast lithology (Sweet and Soreghan, 2010) and detrital zircon spectra (Leary et al., 2020). Detrital zircon data from the Kerber and Sharpsdale formations, located ~20 km to the north of our study area, show a consistently dominant ca. 1.7 Ga mode but a decrease and disappearance of lesser Archean, Mesoproterozoic, and Paleozoic modes upsection (Leary et al., 2020). A different trend is observed within our study area, where paleocurrent data and detrital zircon age distributions are consistent throughout this stage (Fig. 3A), suggesting that recycled sediment from the south was itself initially sourced by the same (or similar) basement terrane that was being unroofed. The recycled sedimentary sources were not substantively composed of Mississippian rocks, because they are mostly carbonate, and the minor sandstones within these carbonates bear different detrital zircon spectra than those in Early–Middle Pennsylvanian strata (Fig. 3A) (Leary et al., 2020; sample BC05). Pierce (1969) suggested Devonian through Cambrian formations as potential sedimentary sources, but Neoproterozoic sedimentary and metasedimentary rocks around western Laurentia also contain corresponding age modes (Matthews et al., 2018) that could have been contributed to Central Colorado Trough strata.

Based on detrital-zircon age distributions from our study area, the sedimentary and then basement rock that sourced Lower–Middle Pennsylvanian strata contained predominantly ca. 1.67 Ga zircons, but also minor ca. 1.43 Ga zircons and even fewer of Cambrian age. The contribution of this minor population of Cambrian detrital zircon was likely either directly sourced or recycled from late Neoproterozoic and early Paleozoic strata (Matthews et al., 2018) that itself was originally sourced from a Wet Mountains–like intrusion. This interpretation is consistent with low εHf(t) values and a mix of REE patterns in detrital zircons, some of which lack negative Eu anomalies.

Paleocurrents throughout the basin support northeastward sediment transport from the Uncompahgre Uplift (Fig. 10; Hoy and Ridgeway, 2002; Musgrave, 2003). Musgrave (2003) suggested that coarse-grained material within our study area was contributed by highlands to the east, although no paleocurrent data support this. Deposition of the Kerber and Sharpsdale formations occurred in both marine and terrestrial environments, which included braided fluvial and deltaic systems, coal-forming swamps, and shallow marine carbonate shelves (Brill, 1952; Peel, 1971; De Voto and Peel, 1972; Musgrave, 2003). The transgressions and regressions of these environments were driven by fluctuations in eustatic sea level and tectonics (Blakey, 2009). As subsidence rates in many other Ancestral Rocky Mountain basins increased (Sweet et al., 2021), accommodation creation along the western thrusted margin of the Central Colorado Trough during Minturn Formation deposition often matched sediment supply, which resulted in aggradational stratal stacking (Hoy and Ridgeway, 2003). Depositional systems at this time were dominated by fan-deltas along basin margins and turbidities farther out in the basin (Lindsey et al., 1986; Hoy and Ridgeway, 2002, 2003). Upper Minturn Formation evaporitic deposits are

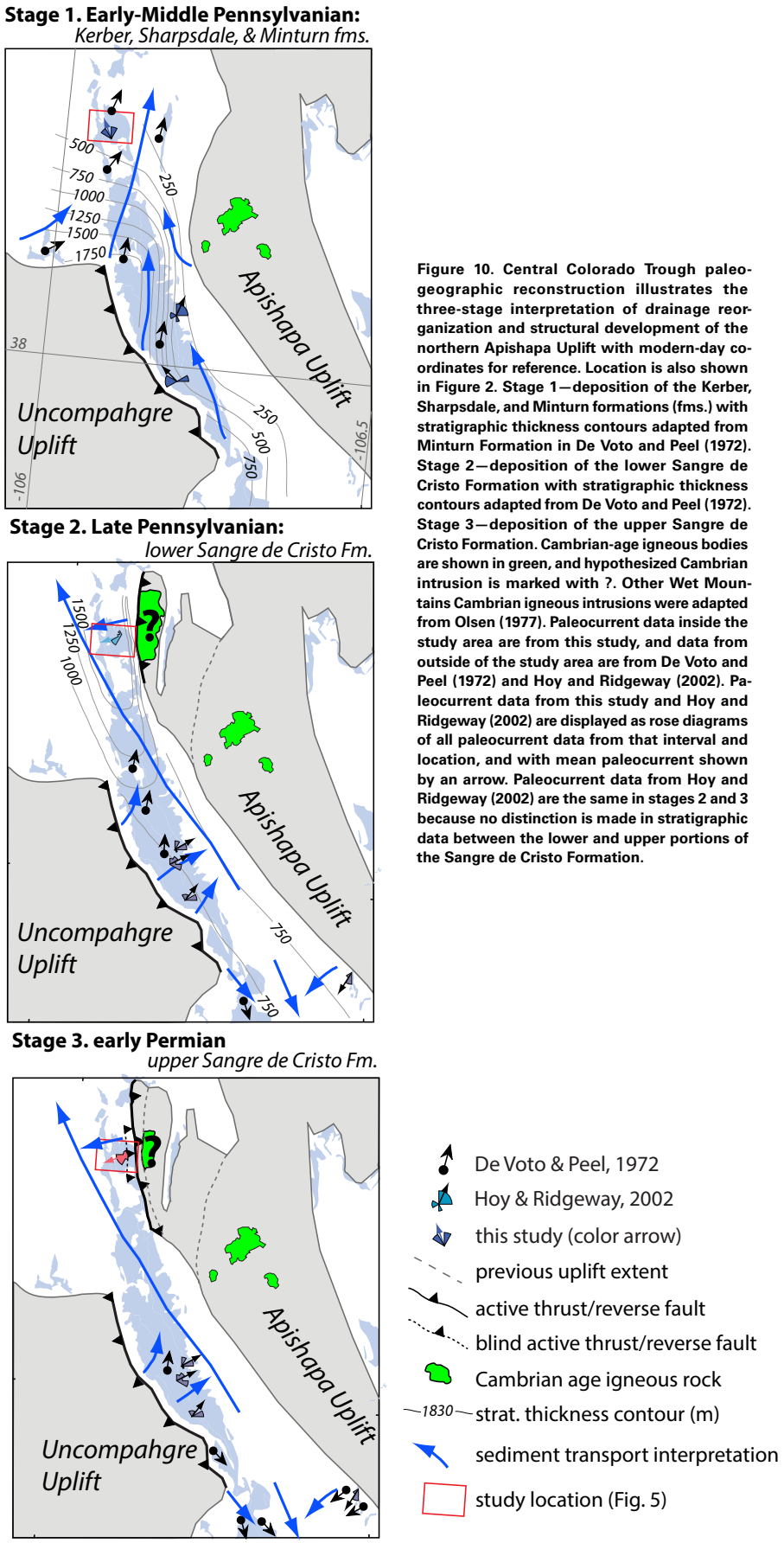

Figure 10. Central Colorado Trough paleogeographic reconstruction illustrates the three-stage interpretation of drainage reorganization and structural development of the northern Apishapa Uplift with modern-day coordinates for reference. Location is also shown in Figure 2. Stage 1—deposition of the Kerber, Sharpsdale, and Minturn formations (fms.) with stratigraphic thickness contours adapted from Minturn Formation in De Voto and Peel (1972). Stage 2—deposition of the lower Sangre de Cristo Formation with stratigraphic thickness contours adapted from De Voto and Peel (1972). Stage 3—deposition of the upper Sangre de Cristo Formation. Cambrian-age igneous bodies are shown in green, and hypothesized Cambrian intrusion is marked with ?. Other Wet Mountains Cambrian igneous intrusions were adapted from Olsen (1977). Paleocurrent data inside the study area are from this study, and data from outside of the study area are from De Voto and Peel (1972) and Hoy and Ridgeway (2002). Paleocurrent data from this study and Hoy and Ridgeway (2002) are displayed as rose diagrams of all paleocurrent data from that interval and location, and with mean paleocurrent shown by an arrow. Paleocurrent data from Hoy and Ridgeway (2002) are the same in stages 2 and 3 because no distinction is made in stratigraphic data between the lower and upper portions of the Sangre de Cristo Formation.

interpreted as an indication of marine restriction (Musgrave, 2003) prior to Sangre de Cristo Formation fluvial deposition.

Stage 2 is marked by a dramatic change in the northern Central Colorado Trough sediment source that occurred between the Minturn (late Stage 1) and lower Sangre de Cristo formations (Figs. 3 and 10). This stage also marks a change in the northern Central Colorado Trough subsidence pattern, with the thickest stratal interval moving from the basin center (Lower–Middle Pennsylvanian) to the eastern edge, adjacent to the Apishapa Uplift (Fig. 8; De Voto and Peel, 1972). We interpret this to indicate tectonically driven exhumation of, and flexural loading by, the northern Apishapa Uplift within the vicinity of our study area. This increase in accommodation in the northern Central Colorado Trough is approximately coeval with a continued high subsidence rate in the Eagle Basin, and increased subsidence rates in many Ancestral Rocky Mountain basins, which include the Paradox, Orogrande, and Pedregosa basins (Fig. 1; Sweet et al., 2021). Deformation on this front is further supported by angular unconformity on, and folding of, the lower Sangre de Cristo Formation within our study area (Fig. 5; Hoy and Ridgeway, 2002).

Feldspar abundance peaked during this stage, and zircon samples exhibit a unimodal Cambrian age source (i.e., 1SMST9 and 2SMST112; Fig. 2B). Zircon εHf(t) and REE composition support a model of sediment sourcing of our study area by a western Laurentian Cambrian granitoid source (Figs. 4 and 7B and 7C). Paleocurrents indicate that this source was to the east, sandstone composition indicates that the source was microcline-rich, and the homogenous detrital zircon Cambrian spectra suggest that the catchment was proximal and did not include notable exposures of zircon-fertile Proterozoic basement. For all of these reasons, we have proposed the presence of a Cambrian igneous sediment source on the western edge of the northern Apishapa Uplift (Fig. 10) that was exposed during this time but that does not presently outcrop. The transverse fluvial system within our study area, perhaps in concert with effects of the Sawatch Uplift, shunted the larger axial fluvial system to the west but most likely did not block it or overwhelm its detrital zircon signature, as no similar age strata in the Eagle Basin exhibit a dominantly Cambrian age mode (Leary et al., 2020). Increased accommodation within our study area, which would have captured more of the local detrital zircon signal rather than allowing it to bypass into the axial system running north, may have also contributed to the lack of a Cambrian zircon observed in the Eagle Basin (Leary et al., 2020). Regardless, at a minimum estimate, the >1.8-km-thick lower Sangre de Cristo Formation in the vicinity of the study area (Fig. 5) documents a large volume of Cambrian-sourced detritus that was produced by the northern Apishapa Uplift and dominated the sedimentary record for ~5 m.y.

Stage 3 marks further drainage reorganization within our study area that occurred across the well-mapped angular unconformity between the upper and lower Sangre de Cristo Formation, and which exhibits a decrease in discordance to the west (Fig. 5; Pierce, 1969; De Voto et al., 1971; Taylor et al., 1975; Wallace et al., 2000; Hoy and Ridgeway, 2002). This feature documents a continuation and basinward migration of northern Apishapa Uplift deformation (Fig. 8A) during the Late Pennsylvanian–early Permian that was coeval with a shift in provenance.

On the eastern edge of the study area, lower Sangre de Cristo Formation strata turn almost vertical to meet the base of the upper Sangre de Cristo Formation (Fig. 5), which suggests that >1 km of strata were locally exhumed prior to deposition of the upper Sangre de Cristo Formation. Detrital zircon data show a prominent Cambrian mode in the upper Sangre de Cristo Formation, but it is supplanted by a dominant bimodal distribution of Proterozoic ages (Fig. 3A). The sandstone sample that corresponds to this detrital zircon spectra indicates a modest increase in quartz content (Fig. 3B). Mean sediment transport direction during this time was still west-southwest, but the distribution of paleoflow measurements is broader than in the lower Sangre de Cristo Formation (Figs. 3A and 10). Based on the introduction of the Proterozoic age modes and high feldspar abundance, the newly exhumed source area during this stage was basement of common Laurentian crustal affinity. However, the Cambrian detrital signal may be either basement derived or recycled from the folded and eroded lower Sangre de Cristo Formation. The similarity of zircon εHf(t) and REE of the upper and lower Sangre de Cristo Formation (Fig. 7A–7C) is not useful in discriminating between these two scenarios. During this stage, regional axial sediment transport (Hoy and Ridgeway, 2002) continued, and sediment transport within the study area remained transverse, albeit with a source area that had migrated closer to, and partly within, the depocenter (Fig. 10).

CONCLUSIONS

Using the Central Colorado Trough as a case study, this study emphasizes the power of integrating zircon petrochronology as part of a multi-proxy data set for provenance reconstruction. Although multiple sedimentary sources yield zircons of similar Cambrian U-Pb ages, Hf isotopes and REE abundances provided a basis for discriminating between these otherwise ambiguous sources. Zircon εHf(t) values from Cambrian igneous rocks contributed a regional diagnostic provenance tool due to an east-to-west decrease in Hf isotopic ratios observed in potential sediment sources. Conversely, detrital zircon REE abundances and ratios provided a tool for discriminating between different local sources based on the mineralogical composition of source rocks as suggested by Belousova et al. (2002). Along with paleocurrent, sediment thickness, and structural data, zircon petrochronology indicates that the dominant source of Cambrian detrital zircons in the Central Colorado Trough is no longer exposed. Therefore, the only known record of this igneous body is in the basin, which preserves the mineralogic and chemical signature of the now-missing Cambrian intrusion(s). Furthermore, the implications of these data bear on how Cambrian detrital zircons in North American stratigraphy are interpreted and to what source(s) they are attributed.

Based on the provenance reconstruction, we present a three-stage tectonic activity and drainage reorganization model for the northern Central Colorado Trough, which integrates previous work throughout the basin and Ancestral Rocky Mountains. Stage 1 depicts the initial development of the northern

Central Colorado Trough as a depocenter in the Early–Middle Pennsylvanian, exhumation and unroofing of sedimentary source rock down to the basement, and northward sediment dispersal through our study area. Stage 2 occurred during the Late Pennsylvanian, when fluvial deposition throughout the Central Colorado Trough became dominant (Hoy and Ridgeway 2002, 2003), and within our study area paleocurrents rotated to the west–southwest and detrital zircons were supplied by proximal Cambrian igneous rocks. This Cambrian igneous body was exhumed on the northern end of the Apishapa Uplift. Stage 3 is marked by continued, basinward migration of the northwestern Apishapa deformation front, which drove development of an angular unconformity and the addition of bimodal Proterozoic age distribution, which relegated the Cambrian age mode to a secondary source. In both stages 2 and 3 (Late Pennsylvanian–early Permian), the northern Central Colorado Trough received sediment from restricted catchments directly to the east of the basin and was isolated from not just continental, but regional, sediment sources. This high degree of isolation was the direct result of tectonic activity in the adjacent Apishapa Uplift.

ACKNOWLEDGMENTS

Field and lab work were funded by the National Science Foundation (EAR-1824557) and graduate student grants from the American Association of Petroleum Geologists, the Geological Society of America, Sigma Xi, and the University of Houston. Many thanks go to field assistants Lokin Casturi, Crystal Saadeh, Kenny Lambert, and Noah Karsky. Special thanks go to Minako Righter and Yongjun Gao for assisting with the U-Pb and Hf isotopic and trace-elemental abundance analyses and maintaining the University of Houston LA-ICP-MS and MC-ICP-MS lab facilities. Thanks go to the Wichita Mountain Wildlife Refuge for granting sampling access within the refuge. This manuscript greatly benefited from constructive edits by David Malone and Dustin Sweet.

REFERENCES CITED

Aleinikoff, J.N., Zartman, R.E., Walter, M., Rankin, D.W., Lyttle, P.T., and Burton, W.C., 1995, U-Pb ages of metarhyolites of the Catoctin and Mount Rogers formations, central and southern Appalachians: Evidence for two phases of lapetan rifting: American Journal of Science, v. 295, p. 428–454, https://doi.org/10.2475/ajs.295.4.428.

Alexander, J.E.C., Mickelson, G.M., and Lanphere, M.A., 1978, MMhb-1: A new ^{40}Ar-^{39}Ar dating standard, *in* Zartman, R.E., ed., Short Papers of the Fourth International Conference, Geochronology, Cosmochronology, and Isotope Geology: U.S. Geological Survey, Open-File Report 78-701, p. 6–8.

Amato, J.M., and Mack, G.H., 2012, Detrital zircon geochronology from the Cambrian–Ordovician Bliss Sandstone, New Mexico: Evidence for contrasting Grenville-age and Cambrian sources on opposite sides of the Transcontinental Arch: Geological Society of America Bulletin, v. 124, no. 11–12, p. 1826–1840, https://doi.org/10.1130/B30657.1.

Aretz, M., Herbig, H.G., and Wang, X.D., 2020, The Carboniferous Period, *in* Gradstein, F.M., Ogg, J.G., Schmitz, M.D., and Ogg, G.M., eds., Geologic Time Scale: Elsevier, p. 811–874.

Armstrong, A.K., Mamet, B.L., and Repetski, J.E., 1992, Stratigraphy of the Mississippian system, south-central Colorado and north-central New Mexico: U.S. Geological Survey Bulletin 1787-E, 22 p.

Baltz, E.H., and Meyers, D.A., 1999, Stratigraphic framework of upper Paleozoic rocks, southeastern Sangre de Cristo Mountains, New Mexico: New Mexico Bureau of Mines and Mineral Resources Memoir 48, 269 p.

Baltz, E.H., and O'Neill, M., 1980, Preliminary geologic map of the Mora River area, Sangre de Cristo Mountains, New Mexico: U.S. Geological Survey Open-File Map 80–374.

Barbeau, D.L., 2003, A flexural model for the Paradox Basin: Implications for the tectonics of the Ancestral Rocky Mountains: Basin Research, v. 15, no. 1, p. 97–115, https://doi.org/10.1046/j.1365-2117.2003.00194.x.

Belousova, E.A., Griffin, W.L., O'Reilly, S.Y., and Fisher, N.I., 2002, Igneous zircon: Trace element composition as an indicator of source rock type: Contributions to Mineralogy and Petrology, v. 143, p. 602–622, https://doi.org/10.1007/s00410-002-0364-7.

Belousova, E.A., Kostitsyn, Y.A., Griffin, W.L., Begg, G.C., O'Reilly, S.Y., and Pearson, N.J., 2010, The growth of continental crust: Constraints from zircon Hf-isotope data: Lithos, v. 119, p. 457–466, https://doi.org/10.1016/j.lithos.2010.07.024.

Bickford, M., Van Schmus, W.R., Karlstrom, K.E., Mueller, P.A., and Kamenov, G.D., 2015, Mesoproterozoic–trans-Laurentian magmatism: A synthesis of continent-wide age distributions, new SIMS U–Pb ages, zircon saturation temperatures, and Hf and Nd isotopic compositions: Precambrian Research, v. 265, p. 286–312, https://doi.org/10.1016/j.precamres.2014.11.024.

Blakey, R.C., 2009, Paleogeography and geologic history of the Western Ancestral Rocky Mountains, Pennsylvanian–Permian, southern Rocky Mountains and Colorado Plateau, *in* Houston, W.S., Wray, L.L., and Moreland, P.G., eds., The Paradox Basin Revisited—New Developments in Petroleum Systems and Basin Analysis: Rocky Mountain Association of Geologists Special Publication, p. 222–264.

Bouvier, A., Vervoot, J.D., and Patchett, P.J., 2008, The Lu–Hf and Sm–Nd isotopic composition of CHUR: Constraints from unequilibrated chondrites and implications for the bulk composition of terrestrial planets: Earth and Planetary Science Letters, v. 273, p. 48–57, https://doi.org/10.1016/j.epsl.2008.06.010.

Brill, K.G., Jr., 1952, Stratigraphy in the Permo-Pennsylvanian Zeugeosyncline of Colorado and Northern New Mexico: Geological Society of America Bulletin, v. 63, p. 809–880, https://doi.org/10.1130/0016-7606(1952)63[809:SITPZO]2.0.CO;2.

Carlson, M.P., 1999, Transcontinental Arch—A pattern formed by rejuvenation of local features across central North America: Tectonophysics, v. 305, p. 225–233, https://doi.org/10.1016/S0040-1951(99)00005-0.

Chowdhury, N.U.M.K., and Sweet, D.E., 2020, Subsurface stratigraphy and basin-fill architecture of the late Paleozoic eastern Taos Trough, northern New Mexico, U.S.A.: The Mountain Geologist, v. 57, p. 149–176, https://doi.org/10.31582/rmag.mg.57.3.149.

De Voto, R.H., 1980, Pennsylvanian stratigraphy and history of Colorado, *in* Kent, H.C., and Porter, K.W., eds., Colorado Geology: Denver, Colorado, Rocky Mountain Association of Geologists, p. 71–101.

De Voto, R.H., and Peel, F.A., 1972, Pennsylvanian and Permian stratigraphy and tectonism in central Colorado: Colorado School of Mines Quarterly, v. 67, no. 4, p. 139–185.

De Voto, R.H., and Pierce, W.H., 1971, Pennsylvanian and Permian stratigraphy, tectonism, and history, northern Sangre de Cristo Range, Colorado: New Mexico Geological Society 22nd Annual Fall Field Conference Guidebook, p. 141–163.

De Voto, R.H., Bartleson, B.L., Schenk, C.J., and Waechter, N.B., 1986, Late Paleozoic stratigraphy and Syndepositional tectonism, northwestern Colorado, *in* New Interpretations of Northwest Colorado Geology: Rocky Mountain Association of Geologists Symposium–1986, p. 37–50.

DeCelles, P.G., Langford, R.P., and Schwartz, R.K., 1983, Two new methods of paleocurrent determination from trough cross-stratification: Journal of Sedimentary Research, v. 53, no. 2, p. 629–642.

Degeller, M., Wright, J.E., Hogan, J.P., Gilbert, M.C., and Price, J.D., 1996, Age and source characteristics of Mount Scott Granite, Oklahoma: Geological Society of America Abstracts with Programs, v. 28, no. 1, p. 10.

Dickinson, W.R., Gehrels, G.E., and Stern, R.J., 2010, Late Triassic Texas Uplift preceding Jurassic opening of the Gulf of Mexico: Evidence from U-Pb ages of detrital zircons: Geosphere, v. 6, no. 5, p. 641–662, https://doi.org/10.1130/GES00532.1.

Ejembi, J.I., Potter-McIntyre, S.L., Sharman, G.R., Smith, T.M., Saylor, J.E., Hatfield, K., and Ferré, E.C., 2021, Detrital zircon geochronology and provenance of the Middle to Late Jurassic Paradox Basin and Central Colorado Trough: Paleogeographic implications for southwestern Laurentia: Geosphere, v. 17, p. 1494–1516, https://doi.org/10.1130/GES02264.1.

Fanning, M.C., and Link, P.K., 2004, U-Pb SHRIMP ages of Neoproterozoic (Sturtian) glaciogenic Pocatello Formation, southeastern Idaho: Geology, v. 32, no. 10, p. 881–884, https://doi.org/10.1130/G20609.1.

Folk, R.L., 1974, Petrology of Sedimentary Rocks: Austin, Hemphill Publishing Company, 184 p.

Frahme, C.W., and Vaughn, E.B., 1983, Paleozoic geology and seismic stratigraphy of the northern Uncompahgre Front, Grand County, Utah, *in* Lowell, J.D., and Gries, R., eds., Rocky Mountain Foreland Basins and Uplifts: Rocky Mountain Association of Geologists, p. 201–211.

Freeman, V.L., and Bryant, B., 1977, Red bed formations in the Aspen region, Colorado, *in* Veal, H.K., ed., Exploration Frontiers of the Central and Southern Rockies: Rocky Mountain Association of Geologists, p. 181–189.

Freiburg, J.T., Holland, M.E., Malone, D.H., and Malone, S.J., 2020, Detrital zircon geochronology of basal Cambrian strata in the deep Illinois Basin, USA: Evidence for the Paleoproterozoic–Cambrian Tectonic and Sedimentary Evolution of Central Laurentia: The Journal of Geology, v. 128, https://doi.org/10.1086/708432.

Goodge, J.W., and Vervoort, J.D., 2006, Origin of Mesoproterozoic A-type granites in Laurentia: Hf isotopic evidence: Earth and Planetary Science Letters, v. 243, p. 711–731, https://doi.org/10.1016/j.epsl.2006.01.040.

Green, G.N., 1992, The digital map of Colorado in ARC/INFO format: U.S. Geological Survey Open-File Report 92-0507.

Guitreau, G., Mukasa, S.B., Blichert-Toft, J., and Fahnestock, M.F., 2016, Pikes Peak Batholith (Colorado, USA) revisited: A SIMS and LA-ICP-MS study of zircon U–Pb ages combined with solution Hf isotopic compositions: Precambrian Research, v. 280, p. 179–194, https://doi.org/10.1016/j.precamres.2016.05.001.

Hames, W.E., Hogan, J.P., and Gilbert, M.C., 1998, Revised granite-gabbro age relationships, Southern Oklahoma Aulacogen, U.S.A., *in* Hogan, J.P., and Gilbert, M.C., eds., Basement Tectonics 12: Proceedings of the Twelfth International Conference on Basement Tectonics: Dordrecht, The Netherlands, Kluwer, p. 247–249.

Hanson, R.E., and Eschberger, A.M., 2014, An overview of the Carlton Rhyolite Group: Cambrian A-type felsic volcanism in the Southern Oklahoma Aulacogen: Oklahoma Geologic Survey Guidebook 38, p. 123–142.

Hanson, R.E., Puckett, R.E., Jr., Keller, G.R., Brueseke, M.E., Bulen, C.L., Mertzman, S.A., Finegan, S.A., and McCleery, D.A., 2013, Intraplate magmatism related to opening of the southern Iapetus Ocean: Cambrian Wichita igneous province in the Southern Oklahoma rift zone: Lithos, v. 174, p. 57–70, https://doi.org/10.1016/j.lithos.2012.06.003.

Henderson, C.M., and Shen, S.Z., 2020, The Permian Period, *in* Gradstein, F.M., Ogg, J.G., Schmitz, M.D., and Ogg, G.M., eds., Geologic Time Scale: Elsevier, p. 875–902.

Hoffman, P., Dewey, J.F., and Burke, K., 1974, Aulacogens and their genetic relation to geosynclines, with a Proterozoic example from Great Slave Lake, Canada, *in* Dott, R.H., Jr., and Shaver, R.H., eds., Modern and Ancient Geosynclinal Sedimentation: Society of Economic Paleontologists and Mineralogists Special Publication 19, p. 38–55.

Hogan, J.P., Gilbert, M.C., Price, J.D., and Wright, J.E., 1995, Petrogenesis of A-type sheet granites from an ancient rift, *in* Brown, M., and Piccoli, P.M., eds., The Origin of Granites and Related Rocks: Third Hutton Symposium Abstracts: U.S. Geological Survey Circular 1129, p. 68–69.

Houck, K.J., 1991, Structural control on distribution of sedimentary facies in the Pennsylvanian Minturn Formation of northcentral Colorado: U.S. Geological Survey Bulletin 1787-Y, 33 p.

Hoy, R.G., 2000, Syndepositional deformation, sedimentation, and regional tectonics of an Ancestral Rocky Mountains Basin, Central Colorado Trough, Colorado [Ph.D. thesis]: West Lafayette, Indiana, Purdue University, 252 p.

Hoy, R.G., and Ridgeway, K.D., 2002, Syndepositional thrust-related deformation and sedimentation in an Ancestral Rocky Mountains Basin, Central Colorado Trough, Colorado, USA: Geological Society of America Bulletin, v. 114, no. 7, p. 804–828, https://doi.org/10.1130/0016-7606(2002)114<0804:STRDAS>2.0.CO;2.

Hoy, R.G., and Ridgeway, K.D., 2003, Sedimentology and sequence stratigraphy of fan delta and river-delta deposystems, Pennsylvanian Minturn Formation, Colorado: American Association of Petroleum Geologists Bulletin, v. 87, no. 7, p. 1169–1191.

Johnson, S.Y., Chan, M.A., and Konopka, E.A., 1992, Pennsylvanian and Early Permian paleogeography of the Unita-Piceance Basin region, northwestern Colorado and northeastern Utah: U.S. Geological Survey Bulletin 1787, 35 p.

Kampunzu, A.B., and Mohr, P., 1991, Magmatic evolution and petrogenesis in the East African Rift, *in* Kampunzu, A.B., and Lubala, R.T., eds., Magmatism in Extensional Structural Settings: The Phanerozoic African Plate: Berlin, Heidelberg, Springer, p. 85–136, https://doi.org/10.1007/978-3-642-73966-8_5.

Keller, G.R., and Stephenson, R.A., 2007, The southern Oklahoma and Dnieper-Donets aulacogens: A comparative analysis, *in* Hatcher, R.D., Carlson, M.P., McBride, J.H., and Martínez Catalán, J.R., eds., 4-D Framework of Continental Crust: Geological Society of America Memoir 200, p. 127–143, https://doi.org/10.1130/2007.1200(08).

Kluth, C., 1997, Comparison of the location and structure of the late Paleozoic and Late Cretaceous-early Tertiary Front Range Uplift: Colorado Front Range Guidebook–1997, p. 31–42.

Kluth, C.F., 1986, Plate tectonics of the Ancestral Rocky Mountains, *in* Peterson, J.A., ed., Paleotectonics and Sedimentation in the Rocky Mountain Region, United States: American Association of Petroleum Geologists Memoir 41, p. 353–369, https://doi.org/10.1306/M41456C17.

Kluth, C.F., and Coney, P.J., 1981, Plate-tectonics of the Ancestral Rocky Mountains: Geology, v. 9, no. 1, p. 10–15, https://doi.org/10.1130/0091-7613(1981)9<10:PTOTAR>2.0.CO;2.

Kottlowski, F.E., 1961, Pennsylvanian rocks in north-central New Mexico, *in* Northrop, S.A., ed., Albuquerque Country: New Mexico Geological Society, 12th Field Conference Guidebook, p. 97–104.

Larson, E.E., Patterson, P.E., Curtis, G., Drake, R., and Mutschler, F.E., 1985, Petrologic, paleomagnetic, and structural evidence of a Paleozoic rift system in Oklahoma, New Mexico, Colorado and Utah: Geological Society of America Bulletin, v. 96, p. 1364–1372, https://doi.org/10.1130/0016-7606(1985)96<1364:PPASEO>2.0.CO;2.

Lawton, T.F., Cashman, P.H., Trexler, J.H., and Taylor, W.J., 2017, The late Paleozoic Southwestern Laurentian Borderland: Geology, v. 45, no. 8, p. 675–678, https://doi.org/10.1130/G39071.1.

Leary, R.J., Umhoefer, P., Smith, M.E., and Riggs, N., 2017, A three-sided orogen: A new tectonic model for Ancestral Rocky Mountain Uplift and Basin development: Geology, v. 45, no. 8, p. 735–738, https://doi.org/10.1130/G39041.1.

Leary, R.J., Umhoefer, P., Smith, M.E., Smith, T.M., Saylor, J.E., Riggs, N., Burr, G., Lodes, E., Foley, D., Licht, A., Mueller, M.A., and Baird, C., 2020, Provenance of Pennsylvanian–Permian sedimentary rocks associated with the Ancestral Rocky Mountains orogeny in southwestern Laurentia: Implications for continental-scale Laurentian sediment transport systems: Lithosphere, v. 12, p. 88–121, https://doi.org/10.1130/L1115.1.

Linde, G.M., Cashman, P.H., Trexler, J.H., and Dickinson, W.R., 2014, Stratigraphic trends in detrital zircon geochronology of upper Neoproterozoic and Cambrian strata, Osgood Mountains, Nevada, and elsewhere in the Cordilleran miogeocline: Evidence for Early Cambrian uplift of the Transcontinental Arch: Geosphere, v. 10, no. 6, p. 1402–1410, https://doi.org/10.1130/GES01048.1.

Lindsey, D.A., Clark, R.P., and Soulliere, S.J., 1986, Minturn and Sangre de Cristo Formations of southern Colorado: A prograding fan-delta and alluvial fan sequence shed from the Ancestral Rocky Mountains, *in* Peterson, J.A., ed., Paleotectonics and Sedimentation: American Association of Petroleum Geologists Memoir 41, p. 541–561, https://doi.org/10.1306/M41456C26.

Link, P.K., Todt, M.K., Pearson, D.M., and Thomas, R.C., 2017, 500–490 Ma detrital zircons in Upper Cambrian Worm Creek and correlative sandstones, Idaho, Montana, and Wyoming: Magmatism and tectonism within the passive margin: Lithosphere, v. 9, no. 6, p. 910–926, https://doi.org/10.1130/L671.1.

Marshak, S., Karlstrom, K., and Timmons, J.M., 2000, Inversion of Proterozoic extensional faults: An explanation for the pattern of Laramide and Ancestral Rockies intracratonic deformation, United States: Geology, v. 28, no. 8, p. 735–738, https://doi.org/10.1130/0091-7613(2000)28<735:IOPEFA>2.0.CO;2.

Matthews, W., Guest, B., and Madronich, L., 2018, Latest Neoproterozoic to Cambrian detrital zircon facies of western Laurentia: Geosphere, v. 14, no. 1, p. 243–264, https://doi.org/10.1130/GES01544.1.

McConnell, D.A., 1988, Constraints on magnitude and sense of slip across the northern margin of the Wichita Uplift, southwest Oklahoma, *in* Johnson, K.S., ed., Anadarko Basin Symposium, Oklahoma Geological Survey Circular 90, p. 85–96.

McMillan, N.J., and McLemore, V.T., 2004, Cambrian–Ordovician magmatism and extension in New Mexico and Colorado: New Mexico Bureau of Geology and Mineral Resources Bulletin, v. 160, p. 1–11.

McMillan, N.J., Dickin, A.P., and Haag, D., 2000, Evolution of magma source regions in the Rio Grande rift, southern New Mexico: Geological Society of America Bulletin, v. 112, no. 10, p. 1582–1593, https://doi.org/10.1130/0016-7606(2000)112<1582:EOMSRI>2.0.CO;2.

Musgrave, B.E., 2003, Lower Pennsylvanian stratigraphy of the Central Colorado Trough [M.Sc. thesis]: Lubbock, Texas, Texas Tech University, 150 p.

Myrow, P.M., Lukens, C., Lamb, M.P., Houck, K., and Strauss, J., 2008, Dynamics of a transgressive prodeltaic system: Implications for geography and climate within a Pennsylvanian intracratonic basin, Colorado, U.S.A.: Journal of Sedimentary Research, v. 78, p. 512–528, https://doi.org/10.2110/jsr.2008.061.

Olson, J.C., Marvin, R.F., Parker, R.L., and Mehnert, H.H., 1977, Age and tectonic setting of Lower Paleozoic alkalic and mafic rocks, carbonatites, and thorium veins in south central Colorado: Journal of Research of the U.S. Geological Survey, v. 5, p. 673–687.

Peel, F.A., 1971, New interpretations of Pennsylvanian and Permian stratigraphy and structural history, northern Sangre de Cristo Range, Colorado [M.Sc. thesis]: Golden, Colorado, Colorado School of Mines, 75 p.
Pierce, W.H., 1969, Geology and Pennsylvanian-Permian stratigraphy of the Howard area, Fremont County, Colorado [M.Sc. thesis]: Golden, Colorado, Colorado School of Mines, 129 p.
Powell, B.N., Gilbert, M.C., and Fischer, J.F., 1980, Lithostratigraphic classification of basement rocks of the Wichita province, Oklahoma: Geological Society of America Bulletin, v. 91, p. 509–514 and p. 1875–1994.
Price, J.D., 1998, Petrology of the Mount Scott Granite [Ph.D. dissertation]: Norman, Oklahoma, University of Oklahoma, 240 p.
Rasmussen, D.M., and Foreman, B.Z., 2017, Provenance of lower Paleogene strata in the Huerfano Basin: Implications for uplift of the Wet Mountains, Colorado, U.S.A.: Journal of Sedimentary Research, v. 87, p. 579–593, https://doi.org/10.2110/jsr.2017.30.
Scherer, E.E., Munker, C., and Mezger, K., 2001, Calibration of the lutetium-hafnium clock: Science, v. 293, p. 683–687, https://doi.org/10.1126/science.1061372.
Schoene, B., and Bowring, S.A., 2006, U-Pb systematics of the McClure Mountain syenite: Thermochronological constraints on the age of the $^{40}Ar/^{39}Ar$ standard MMhb: Contributions to Mineral Petrology, v. 151, p. 615–630.
Sláma, J., Košler, J., Condon, D. J., Crowley, J. L., Gerdes, A., Hanchar, J. M., Horstwood, M. S., Morris, G. A., Nasdala, L., and Norberg, N., 2008, Plešovice zircon—A new natural reference material for U–Pb and Hf isotopic microanalysis: Chemical Geology, v. 249, no. 1, p. 1–35, https://doi.org/10.1016/j.chemgeo.2007.11.005.
Söderlund, U., Patchett, P.J., Vervoort, J.D., and Isachsen, C.E., 2004, The ^{176}Lu decay constant determined by Lu-Hf and U-Pb isotope systematics of Precambrian mafic intrusions: Earth and Planetary Science Letters, v. 219, p. 311–324, https://doi.org/10.1016/S0012-821X(04)00012-3.
Soule, D.L., 1992, Precambrian to earliest Mississippian stratigraphy, geologic history, and paleogeography of northwestern Colorado and west-central Colorado: U.S. Geological Survey Bulletin 1787-U, 45 p.
Soreghan, G.S., Keller, G.R., Gilbert, M.C., Chase, C.G., and Sweet, D.E., 2012, Load-induced subsidence of the Ancestral Rocky Mountains recorded by preservation of Permian landscapes: Geosphere, v. 8, no. 3, p. 654–668, https://doi.org/10.1130/GES00681.1.
Soreghan, M.J., Heavens, N., Soreghan, G.S., Link, P.K., and Hamilton, M.A., 2014, Abrupt and high-magnitude changes in atmospheric circulation recorded in the Permian Maroon Formation, tropical Pangaea: Geological Society of America Bulletin, v. 126, no. 3–4, p. 569–584, https://doi.org/10.1130/B30840.1.
Stacey, J.S., and Kramers, J., 1975, Approximation of terrestrial lead isotope evolution by a two-stage model: Earth and Planetary Science Letters, v. 26, no. 2, p. 207–221, https://doi.org/10.1016/0012-821X(75)90088-6.
Sturmer, D.M., Trexler, J.H., Jr., and Cashman, P.H., 2018, Tectonic analysis of the Pennsylvanian Ely-Bird Spring Basin: Late Paleozoic tectonism on the Southwestern Laurentia margin and the distal limit of the Ancestral Rocky Mountains: Tectonics, v. 37, https://doi.org/10.1002/2017TC004769.
Su, Q., Goldberg, S.A., and Fullagar, P.D., 1994, Precise U-Pb zircon ages of Neoproterozoic plutons in the southern Appalachian Blue Ridge and their implications for the initial rifting of Laurentia: Precambrian Research, v. 68, p. 81–95, https://doi.org/10.1016/0301-9268(94)90066-3.
Sun, C., Graff, M., and Liang, Y., 2017, Trace element partitioning between plagioclase and silicate melt: The importance of temperature and plagioclase composition, with implications for terrestrial and lunar magmatism: Geochimica et Cosmochimica Acta, v. 206, p. 273–295, https://doi.org/10.1016/j.gca.2017.03.003.
Sundell, K.E., 2017, U-Pb Toolbox at the University of Houston: An open-source program for reducing and visualizing zircon U-Pb data sets. Computers & Geosciences [Ph.D. thesis]: Houston, Texas, University of Houston.
Sundell, K.E., Saylor, J.E., and Pecha, M., 2019, Provenance and recycling of detrital zircons from Cenozoic Altiplano strata and the crustal evolution of western South America from combined U-Pb and Lu-Hf isotopic analysis, *in* Horton, B.K., and Folguera, A., eds., Andean Tectonics: Elsevier, p. 363–397, https://doi.org/10.1016/B978-0-12-816009-1.00014-9.
Suttner, L.J., and Dutta, P.K., 1986, Alluvial sandstone composition and paleoclimate, I. Framework mineralogy: Journal of Sedimentary Petrology, v. 56, no. 3, p. 329–345.
Sweet, D.E., and Soreghan, G.S., 2010, Late Paleozoic tectonics and paleogeography of the Ancestral Front Range: Structural, stratigraphic, and sedimentologic evidence from the Fountain Formation (Manitou Springs, Colorado): Geological Society of America Bulletin, v. 122, no. 3–4, p. 575–594, https://doi.org/10.1130/B26554.1.
Sweet, D.E., Brotherton, J.J., Chowdhury, N.U.M.K., and Ramsey, C.E., 2021, Tectonic subsidence analysis of the Ancestral Rocky Mountains from the interior to the southern margin: Palaeogeography, Palaeoclimatology, Palaeoecology, v. 576, https://doi.org/10.1016/j.palaeo.2021.110508.
Taylor, R.B., Scott, G.R., and Wobus, R.A., 1975, Reconnaissance geologic map of the Howard quadrangle, central Colorado: U.S. Geological Survey Miscellaneous Investigations Series Map I-892, scale 1:62,500.
Thomas, W.A., 1991, The Appalachian-Ouachita rifted margin of southeastern North America: Geological Society of America Bulletin, v. 103, p. 415–431.
Thomas, W.A., 2007, Pennsylvanian sinistral faults along the southwest boundary of the Uncompahgre Uplift, Ancestral Rocky Mountains, Colorado: Geosphere, v. 3, no. 3, p. 119–132, https://doi.org/10.1130/GES00068.1.
Thomas, W.A., Becker, T.P., Samson, S.D., and Hamilton, M.A., 2004, Detrital zircon evidence of a recycled orogenic foreland provenance for Alleghenian clastic-wedge sandstones: The Journal of Geology, v. 112, p. 23–37, https://doi.org/10.1086/379690.
Thomas, W.A., Tucker, R.D., Astini, R.A., and Denison, R.E., 2012, Ages of pre-rift basement and synrift rocks along the conjugate rift and transform margins of the Argentine Precordillera and Laurentia: Geosphere, v. 8, no. 6, p. 1366–1383, https://doi.org/10.1130/GES00800.1.
Timbel, C.R., 2015, Uncompahgre fault geometry: A seismic, field, and gravity study near Nucla, Colorado, Paradox Basin, USA [M.Sc. thesis]: Golden, Colorado, Colorado School of Mines, 102 p.
Van Achterbergh, E., Ryan, C., Jackson, S.E., and Griffin, W.L., 2001, Data reduction software for LA-ICPMS, *in* Sylvester, P., ed., Laser Ablation-ICPMS: The Earth Sciences: Mineralogical Association of Canada Short Course Handbook 29, p. 239–243.
Van Schmus, W.R., Bickford, M.E., Sims, P.K., Anderson, R.R., Shearer, C.K., and Treves, S.B., 1993, Proterozoic geology of the western midcontinent basement, *in* Van Schmus, W.R., and Bickford, M.E., eds., Transcontinental Proterozoic Provinces, Decade of North American Geology: Boulder, Colorado, Geological Society of America, p. 239–259.
Vaughn, P.P., 1972, More vertebrates, including a new microsaur, from the Upper Pennsylvanian of central Colorado: Contributions in Science: Los Angeles County Museum, no. 223, p. 1–30.
Vermeesch, P., 2018, IsoplotR: A free and open toolbox for geochronology: Geoscience Frontiers, v. 9, p. 1479–1493, https://doi.org/10.1016/j.gsf.2018.04.001.
Waechter, N.B., and De Voto, R.H., 1989, Tectonic-stratigraphic framework and petroleum potential of the late Paleozoic Central Colorado Trough, Northwestern Colorado *in* Lorenz, J.C., and Lucas, S.G., eds., Energy Frontiers in the Rockies: Albuquerque, Rocky Mountain Section of the American Association of Petroleum Geologists and Albuquerque Geological Society, p. 91–100.
Wallace, C.A., Cappa, J.A., and Lawson, A.D., 1997, Geologic map of Salida east quadrangle, Chaffee and Fremont counties, Colorado: Colorado Geological Survey Open-File Report 97–6, scale 1:24,000.
Wallace, C.A., Cappa, J.A., and Lawson, A.D., 1999, Geologic map of the Gribbles Park quadrangle, Park and Fremont counties, Colorado: Colorado Geological Survey Open-File Report 99–3, scale 1:24,000.
Wallace, C.A., Apeland, A.D., and Cappa, J.A., 2000, Geologic map of the Jack Hill Mountain quadrangle, Fremont County, Colorado: Colorado Geological Survey Open-File Report 00–1, scale 1:24,000.
Whitmeyer, S.J., and Karlstrom, K.E., 2007, Tectonic model for the Proterozoic growth of North America: Geosphere, v. 3, no. 4, p. 220–259, https://doi.org/10.1130/GES00055.1.
Woodhead, J., and Hergt, J., 2005, A preliminary appraisal of seven natural zircon materials for in situ isotope determination: Geostandards and Geoanalytical Research, v. 29, no. 2, p. 183–195, https://doi.org/10.1111/j.1751-908X.2005.tb00891.x.
Woodward, L.A., Anderson, O.J., and Lucas, S.G., 1999, Late Paleozoic right-slip faults in the Ancestral Rocky Mountains, *in* Pazzaglia, F.J., and Lucas, S.G., eds., New Mexico Geological Society 50th Annual Fall Field Conference Guidebook, p. 149–152.
Wright, J.E., Hogan, J.P., and Gilbert, M.C., 1996, The Southern Oklahoma aulacogen: Not just another B.L.I.P.: Eos (Transactions, American Geophysical Union), v. 77, no. 46, F845.
Ye, H., Royden, L., Burchfield, C., and Schuepbach, M., 1996, Late Paleozoic deformation of interior North America: The Greater Ancestral Rocky Mountains: The American Association of Petroleum Geologists Bulletin, v. 80, no. 9, p. 1397–1423.
Yonkee, W.A., Dehler, C.D., Link, P.K., Balgord, E.A., Keeley, J.A., Hayes, D.S., Wells, M.L., Fanning, C.M., and Johnston, S.S., 2014, Tectono-stratigraphic framework of Neoproterozoic to Cambrian strata, west-central U.S.: Protracted rifting, glaciation, and evolution of the North American Cordilleran margin: Earth-Science Reviews, v. 136, p. 59–95, https://doi.org/10.1016/j.earscirev.2014.05.004.